Universidad Carlos III de Madrid
www.uc3m.es

Bachelor in Biomedical Engineering

2014-2015

Final Project in

"Evaluation of New Optical Spectroscopic Techniques for Tissue Studies"

Laura Rey Barroso

Tutor

Pablo Acedo Gallardo

Universidad Carlos III de Madrid
www.uc3m.es

Table of contents

1. INTRODUCTION: PROJECT APPROACH
   - 1.1. Context and purpose of the project
   - 1.2. State of the art
     - 1.2.1. Cell counting methods
     - 1.2.2. Spectroscopic studies for the detection of fingerprints related to glucose concentration
   - 1.3. Aim and scope of the work
   - 1.4. Methodology
   - 1.5. Structure of the document

2. BACKGROUND
   - 2.1. Theoretical framework
     - 2.1.1. Frequency domain measurements
       - 2.1.1.1. Synchronous detection
   - 2.2. Application of the theoretical framework to the problem of the cell count
     - 2.2.1. Introductory approach to a previous problem
     - 2.2.2. Adaptation to the problem of cell counting
   - 2.3. Application of the theoretical framework to the detection of glucose-related AEGs fluorescence
     - 2.3.1. Previous problem for the basis of AEGs' fluorescence detection
     - 2.3.2. Adaptation of the previous problem to detect glucose-related AEGs' fluorescence

3. DESCRIPTION OF THE INSTRUMENT
    3.1. Instrumentation for the modulation of light and detection of fluorescence
    3.2. General optical setup for the measurement fluorescence
        3.2.1. Optical setup for the measurement of cellular concentration
        3.2.2. Optical setup for the measurement of AEGs' fluorescence

4. EXPERIMENTAL PROTOCOL
    4.1. Experimental protocol to measure cell concentration
    4.2. Experimental protocol to measure AEGs' fluorescence

5. RESULTS AND CONCLUSIONS
    5.1. Results for the cell count estimation
    5.2. Results for the AEGs' fluorescence detection
    5.3. Conclusions

6. BIBLIOGRAPHY

7. ANNEX
    7.1. Project budget

1. Introduction: Project approach.

1.1. Context and purpose of the project

Imaging techniques have developed very fast and extensively in the past few years, becoming essential for the study of structures, properties and processes in all the fields in science.

Non-invasive tissular studies have become especially popular nowadays because they permit to study processes in vivo, without the alteration of the sample under focus, which were not possible to be studied with the imaging techniques in the past.

Fluorescence spectroscopy is one of the imaging techniques that has been developed towards the non-invasive studies of polymers, inorganic materials, cells and tissues; with the purpose of characterize them [1].

The main objectives of this work have been proposed in order to further investigate about the possibilities of fluorescence spectroscopy and consisted on the evaluation of two different applications.

Although the tittle of the offer is maintained, the focus of the work has changed to the evaluation of the problems that are introduced right after this lines. Both are proposed to be studied at the same time since it is possible to carry out both of them under the same system and with similar methodologies.

The problem of cell counting

The first of the proposed applications consists on the estimation of the cell density or cell count on a culture surface by means of fluorescence spectroscopy.

Many common procedures and assays require that scientists first obtain an accurate count of the number or density of viable cells. Such procedures range from simple cell culture maintenance, such as cell splitting; to quantitative experiments.

For instance, for the management of cell cultures in biological research, it is crucial to obtain an accurate cell density estimation in order to adjust accordingly the amount of reagents and chemicals that are required to be applied in the experiment.

In addition, cell count is essential to evaluate the kinetics of cell growth, to search for pathologies or cancer in medicine. It is also needed in cell therapy, to control the dose of cells administered to a patient.

Other many studies also need to make use of a viable cell count like the titration of cell populations in diagnostics; the in-process controls in industrial bioprocesses, etc. [2].

As it is described in a few paragraphs bellow, in the state of the art there exist different methods that accomplish a calculation of the cellular concentration of a cell culture, but sometimes they can present some drawbacks.

The main disadvantage that these techniques present against current implementations of optical techniques is that they cannot estimate a cell culture density non-invasively.

For this reason, it is interesting to develop a study of fluorescence spectroscopy as a possible new option for cell density estimation, since it is possible to approach any sample non-invasively.

It could be interesting to follow cell kinetics directly in the tissue under study. With optics, tissue samples could be possibly studied in the organ to which they belong.

For instance, an application were this can be useful is in the evaluation of tissue regeneration of an implanted graft tissue in a host organ like for instance, the skin, by following the evolution of the graft in the host [3].

The problem of glucose level estimation

The second of the proposed applications consist on the estimation of the level of glucose in blood plasma with fluorescence spectroscopy.

The pathogenesis of diabetes mellitus is related to a high content of glucose in blood. This high content of blood glucose can affect every system of the body over time, leading to many kinds of complications.

Among the most severe ones, are the neurological complications: risk of stroke, nerve damage and cognitive impairment; vascular degeneration, vision loss and kidney disease [4].

According to the World Health Organization, WHO, in 2014 the global prevalence of diabetes was of a 9% in adults over 18. Prevalence data refers to the number of people that are suffering from the illness in that moment.

In addition, according to the WHO, the number of people that died in 2012 as a direct consequence of diabetes was 1.5 million [5]. Hence, it is a fact that diabetes mellitus is as deadly as common.

Fig. 1: Glucometer. The glucose level can be measured easily at home, but still in an invasive way [6].

Diabetes mellitus under treatment, but also untreated, is a progressive illness; there exists control but not healing and depending on the evolution and the degree of control that can be achieved of hyperglycemia, the deterioration of the person accelerates to a greater or a lesser extent [7].

Hence, the development of diagnostic methods or systems aimed at its monitoring is of a great importance. Any method or system that provides an improvement in the control of the disease and facilitates its follow up, must be taken into consideration.

Therefore, also in this case the use of optical technologies is also interesting in order to ease the control of this illness.

The study in this work is aimed to approach the detection of the native fluorescence of certain contents in blood plasma associated with a high glucose concentration; and is orientated towards the future development of non-invasive sensing methods of the glucose content in blood, without the need of extracting a blood sample.

1.2. State of the art

1.2.1. Cell counting methods

There exist diverse methods for the estimation of the cellular concentration of a cell culture.

From the simplest one to the most sophisticated and recent, all of them are used in the laboratories nowadays, regarding to their advantages, drawbacks and specific applications [8].

Hemocytometer or Counting Chamber

The first and still most used method for cell counting is manual counting with a counting chamber, also known as hemocytometer. The hemocytometer is a piece of glass with two especially gridded compartments that can be filled with a cellular suspension.

A very thin crystal is placed on top of the hemocytometer's chambers. A drop of solution from the cell culture is placed near the edge of the chamber and it enters the chamber by capillarity.

If cell viability is to be determined, trypan blue should be added to the cell suspension (in a 1:1 ratio) prior to addition to the chamber. Trypan blue stains dead cells (in blue) to be distinguished from alive ones.

The microscope is then focused on an area of the counting chamber and the cells are counted under the microscope, as round and white (otherwise, dead) corpuscles.

The counting is generally repeated in similar areas on the grid and the results are averaged.

This is the method that is used in this work to determine the number of cells of the cell cultures under analysis in the laboratory, so it will be described more in deep later in the text. This has been the most commonly used method due to its versatility.

It is the cheapest method of determining cell count and cell density, however it is also the slowest and most tedious, because it depends on the analyst's ability to evaluate different cell attributes regardless of the cell type.

It is time consuming too since only one population of cells can be counted at a time.

Automated Cell Counters

These cell counters were designed to perform an automatic count of cells, by using the same principle as the hemocytometer. They count cells in certain areas of the same kind and average the results.

For this purpose, the cellular concentration needs to be in suspension too, and it is loaded into a chamber which is inserted into the counter.

Some automated counters use fluorescence as the method to distinguish between death and alive cells and to be able to make a count, by the use of common stains. This type of counters distinguish very well the cells among other types of materials in the cell suspension, like for instance, cell debris.

This type of cell counters offer very good results and retrieve them very fast. They are easy to use and reduce the amount of time spent and the effort in counting cells under the microscope that may cause eye strain.

On the other hand, they have some drawbacks too.
The count is not reliable if the cells have a lot of variations in shape or are extremely small and also offer poor results when the number of cells in the suspension is very little.

They are neither able to distinguish among different types of cells if present in the solution.

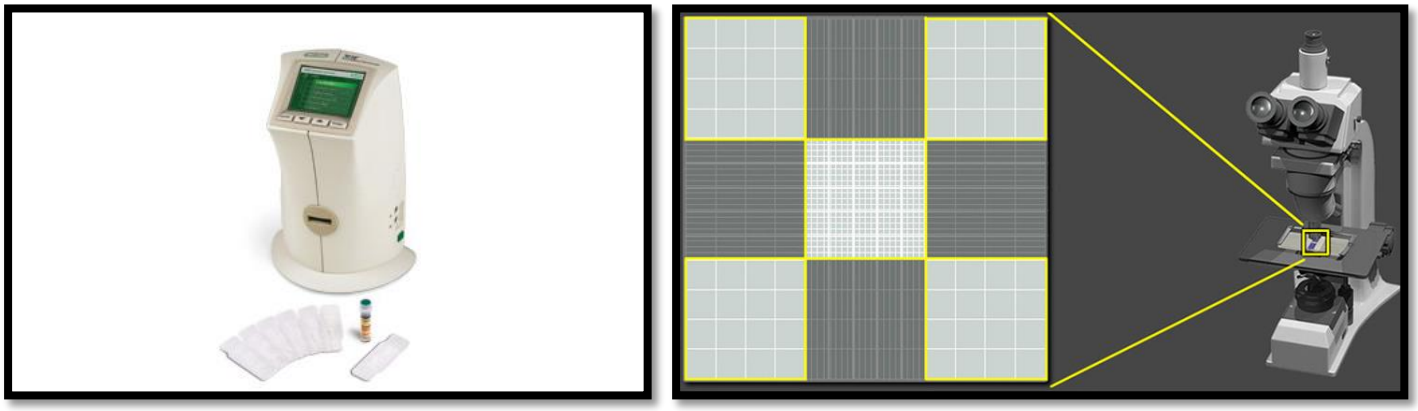

Fig. 2: Automated cell counter (left) and hemocytometer or counting chamber (right) [9, 10].

Coulter counters

Coulter counters are not optical instruments, but rather measure the electrical resistance across a microchannel.

These counters are based on the fact that cells conduct almost no electricity. Two electrodes are placed around the microchannel, in a way that electricity flows unabated, but when a cell is sucked into the gap the current is resisted.

Of course, the cells need to be suspended in a solution and evenly distributed, as in the case of automated cell counters; but in this case a solution without cells needs to be loaded first and then flushed in order to start the count.

On the other hand, it also has some advantages in comparison with automated counters. The change in resistance increases with cell size so with coulter counters it is possible to distinguish among cells of different sizes. Hence, they are used a lot in blood counts in hospitals, where red blood cells and white blood cells need to be quickly and accurately distinguished.

The main drawback of coulter counters is that they do not make a distinction among alive and dead cells, so they are not useful for the type of studies in which cell viability is assessed.

Spectrophotometry

The principle of spectrophotometry is based on the fact that cell suspensions are turbid. This means that they rather absorb or scatter light when light passes through them.

What a spectrophotometer actually measures is the absorbance that a solution of cells has when a light at a certain wavelength is made to fall upon the solution.

The greater the cell density, the less light that will pass through the cuvette where the solution is loaded.

Because it is the only method in which cells are not counted directly but its absorbance of light, other variable components of cell suspensions can affect the measurement. Hence, this one is not a reliable method and enables only an estimation of cell numbers.

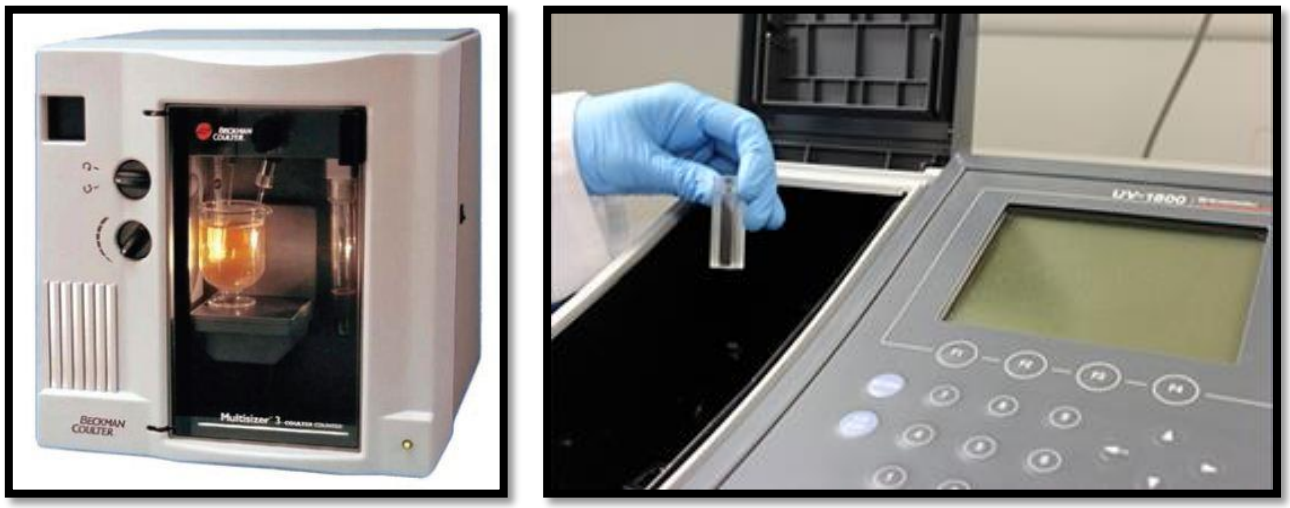

Fig. 3: Coulter counter (on the left) and spectrophotometer [11, 12].

Flow cytometers

They are the best when a detailed cellular analysis is required, as they are able to detect labeling fluorescent components in cells.

Cells flow in a narrow stream in front of a laser beam. The beam hits them one by one, and the light reflected or the fluorescence emitted from the cells is collected to make a cell count of all cells or count different kinds of them.

They can distinguish cells by analyzing their shape and their internal and external structures, as well as measuring the amount of specific proteins and other biochemicals in the cells.

They are very powerful tools but their setup is very expensive and it is not possible to move them from one room to another. They are usually purchased with other purposes than merely analyze cells.

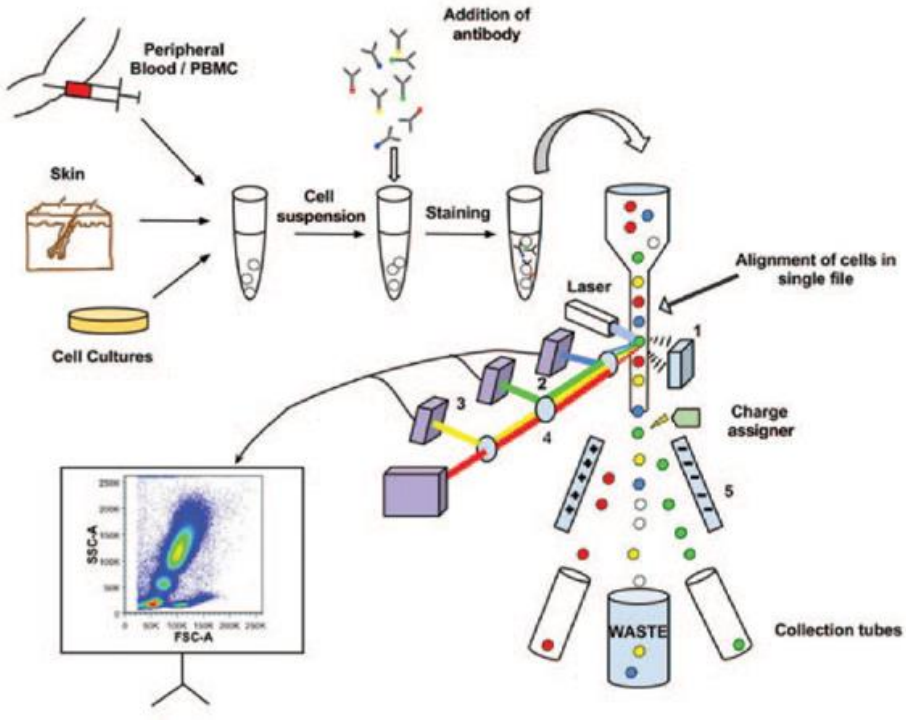

Fig. 4: Flow cytometer equipment (top) and schematic representation of the flow cytometer principle (bottom) [13, 14].

Particular counting methods: Planting

Planting is a counting method that can be used only for colony-forming cells such as bacteria.

In this method, the cells can be simply plated onto a petri dish, heavily diluted with growth medium.

They need to be highly diluted to assume that each cell will give rise to a single colony. The colonies can then be counted, and based on the known volume of culture that was spread on the plate, the cell concentration can be calculated.

All these methods, from the simplest to the most sophisticated one, have advantages and drawbacks that make them optimal for certain purposes.

1.2.2. Spectroscopic studies for the detection of fingerprints related to glucose concentration

In blood, it is possible to find elements that may indicate the presence of different pathologies.

Among those pathologies, it is possible to find the presence of hyperglycemia, characterized for a high glucose level in blood, as explained above.

Several studies relate the presence of high glucose level in blood to the derangement of certain biochemical processes that leave fingerprints for its detection.

For instance, it has been demonstrated that the glycation of certain proteins present in blood plasma is useful to detect the presence of diabetes.

It has been demonstrated that the concentration of glycated albumin, which is produced by the non-enzymatic attachment of glucose to serum albumin, can be use a marker to measure glucose in blood [15].

This has been done by means of analyzing the spectra of drops of albumin with drop coating deposition Raman (DCDR) spectroscopy. DCDR is a particular spectroscopic technique in which a drop of the sample is placed onto a special hydrophobic surface, and then the so called ‘coffee ring effect’ appears with the evaporation of the sample, with the formation of an exterior circular band containing the majority of the sample [16].

In addition, it has also been studied that the absorption coefficient of blood plasma is reduced in the presence diabetes by means of time-domain terahertz spectroscopy [17].

Also the presence of other elements in blood plasma have been demonstrated to be truly related to the presence of glucose; for example certain kind of end products.

With the presence of elevated levels of glucose it is known that advanced glycation end products are formed, also known as AEGs, which come from an accelerated non enzymatic glycation of proteins in blood [18].

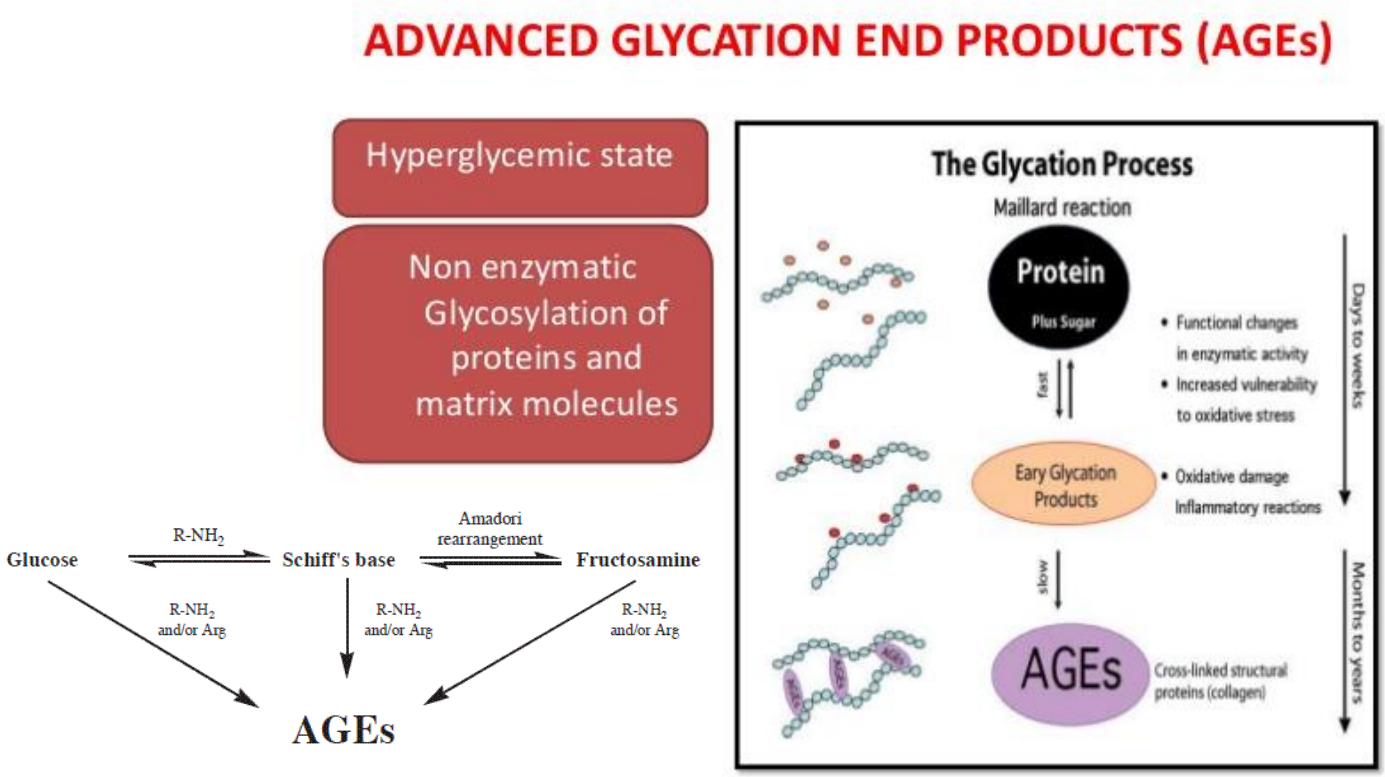

Fig. 5: Nonenzymatic glycosilation is the chemical process by which glucose attaches to proteins and nucleic acids without the aid of enzymes. Within this process, two chemically reversible Schiff base and Amadori product appear adducts form in proportion to glucose concentration. It is known that their accumulation lead to the formation of AEGs. [19, 20]

The presence of AEGs has been demonstrated to be in relation with glucose with an emission spectroscopy analysis of the fluorescence related to this type of glycation end-products [21]. This demonstration is in what the part of glucose detection of this work is going to be based on.

Moreover, the intrinsic fluorescence of proteins has also been attempted to be used in the determination of glucose level [21].
Proteins have also fluorescence themselves, due to tryptophan residues in their structure; and it is known that the conformational changes that proteins suffer affect the fluorescence of tryptophan.

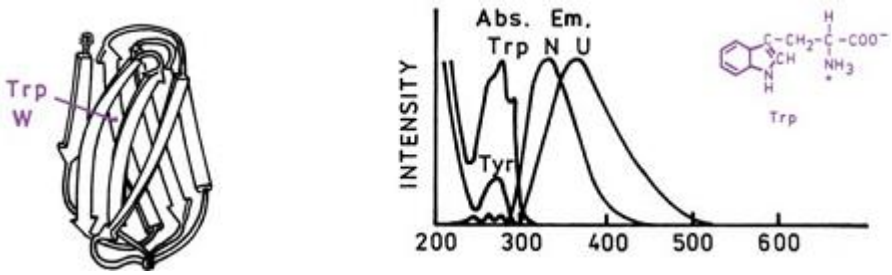

Fig. 6: Emission spectra of Trp residues [22].

When this intrinsic fluorescence of proteins is reduced, it is known that certain pathological processes are going on, and if this fluorescence is significantly reduced it is also known that those pathologies are producing the nonenzymatic glycation of proteins [23, 24].

1.3. Aim and scope of the work

The general aim of the project is to develop an instrument with the principle of fluorescence spectroscopy, which retrieves fluorescence information from the samples under analysis in order to determine different aspects about the samples.

This instrument, although the equipment used in the experimental development is expensive, is aimed to be cheap, compact and portable in the future. And moreover, non-invasive as it was explained a few sections above.

Some of the optical parts that will be described later in the text could even be substituted for 3D-printed affordable versions to make the system even cheaper.

The instrument is going to be evaluated in this work to accomplish cellular concentration determination and detection of the presence of the aforementioned AEGs (whose fluorescence is related to the presence of high glucose levels).

It is known from the bibliography that other metabolites could be used as fingerprints of a high glucose level, but this work is centered in the presence of AEGs because they are very well known to be related to glucose and have been studied before in detail.

The problem of cell counting

The aim of exploring cell counting with this fluorescence spectroscopy instrument is to study the main advantages and drawbacks that we can expect and compare this device with the other ones available.

In this way, analyze if it could contribute to the state of the art and in what kind of applications could it be useful.

The problem of AEGs detection in relation with glucose

The aim of this second study under the developed instrument is to explore the possibilities of obtaining non-invasive measures of glucose in the future, thanks to the fluorescence of certain components in blood (in this case, AEGs) that can be detected with fluorescence spectroscopy.

Common aim

The proposal of both projects has the intention of determining if the method applied is efficient in each case.

Therefore, if it is possible to obtain reliable information from the measurements retrieved. This is carried out by analyzing the data retrieved, to determine if it is truly related with the parameter in question. Finding out the cause of erroneous measurements is crucial, as well as determining if the data appears to be coherent with the characteristics of the source of the detection.

In the scope of this work no further elements for the processing of the data in order to retrieve the actual parameter are included; but the instrument is able to retrieve measurements that can be almost interpreted directly.

1.4. Methodology

The methodology followed in order to carry out both studies is, first the work in the laboratory of optoelectronics. This consist on the installation and connection of all the systems required in the detection of fluorescence.

The equipment for excitation of the sample and the equipment for the collection of the sample's emission is connected and placed around the optics required in each study.

Then, the system is tried for the detection of fluorescence following the steps of a previous reliable study.

Once the system is able to detect reliable measures of fluorescence, the optical system is changed in order to excite and collect the emissions of the samples of interest.

The samples are then obtained in the following ways. For the collection of the different cell populations, the work is translated to the laboratory of

bioengineering, where the samples are obtained in the cell culture room by seeding populations of cells with different concentrations.

Some of the cells are kept in the laboratory in order to obtain more series of samples when needed. This ones, need maintenance during the time that the experiments are carried out, including the change of the medium of growth and the subsequent passes of the culture when this one reaches confluence.

The samples of blood plasma are ordered to another laboratory. They are obtained from mice at the CIEMAT's (Centro de Investigaciones Energéticas, Medioambietales y Tecnológicas) animal facility and brought to the optoelectronics lab properly packed and kept cold for its conservation.

Cell cultures are analyzed the next day after seeding them. Blood plasma samples are analyzed on the same day that they are collected. After their analysis, both kinds of samples are discarded, due to the possible contamination of the samples with the elements in contact, being outside a clean environment.

Several series of cellular concentrations are analyzed on different days, in order to determine if the data that is being obtained is always consistent.

Because the optical system needs to be changed from the cellular samples to the blood plasma ones, it is preferable to make several analyses of just one kind of sample at a time.

After the analysis of cellular concentrations, several series of blood plasma samples with different glucose concentrations are analyzed.

If a source of error, present the data or in the instrumentation is found, its nature is identified and the convenient modifications are made on the system. After including the modifications, following data is analyzed to be truly reliable and able to serve as an indicator of the parameter that is wished to be measured.

1.5. Structure of the document

The document is divided in four main sections, in which all the work involved in this project is described.

In section number two, the theoretical background as well as its application to the detection of fluorescence of the samples are going to be explained.
Then, in the third section it is going to be described the instrument assembled in order to carry out the detection.

Afterwards, in section number four all the steps followed from the collection of the samples until they are ready to be analyzed under the system are going to be explained.

Finally, the results obtained will be presented in the fifth section, as well as the main conclusions taken throughout the development of the project.

2. Background

This chapter introduces theoretical background needed in the development of the detection of fluorescence.

It covers all the theoretical aspects and principles by which the excitation of the samples and the detection of its emission is possible as well as two introductory approaches for the detection of AEGs and cell concentration respectively. This two introductory approaches serve as a guide to apply the theoretical framework to each study.

Afterwards, it is described how they are adapted and how the background is applied to both problems.

2.1. Theoretical framework

Here they are described the principles of spectroscopy on which the experimental applications of this work are based on.

The possibility of creating optical photon interactions with matter when a sample is excited with light is what permits to characterize it by the analysis on how the sample reacts to that light.

This reaction is the combined effect of the sample's absorption and emission of light. In spectroscopy, both absorption and emission of light can be studied.

The emission of samples is studied with emission spectroscopy, where the luminescence occurring from electronically excited states is analyzed. The luminescence of samples can be divided into two categories, depending on the nature of the excited state: fluorescence and phosphorescence.

In fluorescence, the electron which has been promoted to the excited state (by the energy provided of the incident light) has a spin which is opposite to the one of the electron that remains in the ground state, therefore being permitted the relaxation of the excited electron to the ground state.

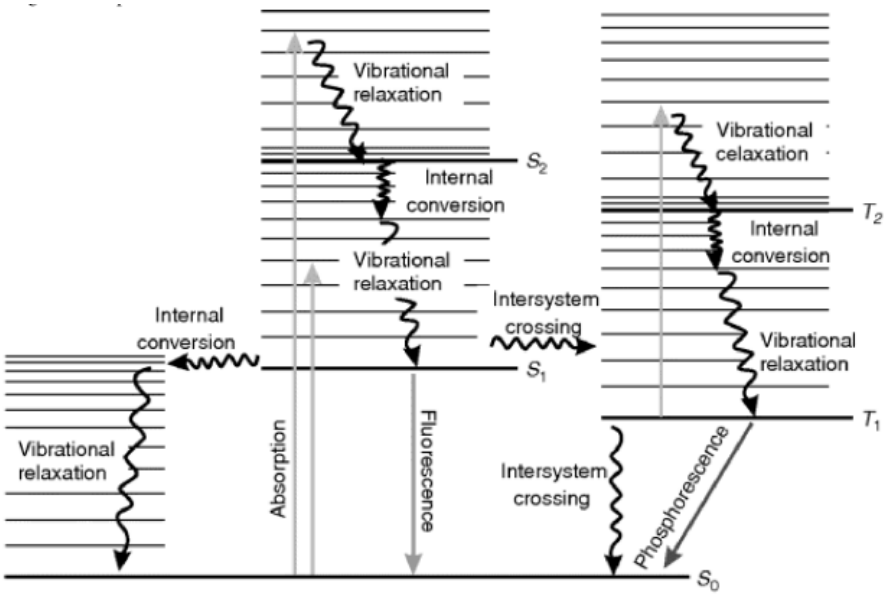

Fig. 7: Phenomena of fluorescence and phosphorescence [1].

This situation is permitted and it is favorable, so consequently, it occurs rapidly, with the emission of a photon by the excited electron. It typically takes just 10 ns for the electron to go from the excited to the ground state, as an average [22].

Despite of the short timescale of fluorescence measurements, with fluorescence spectroscopy it is possible to obtain time-resolved measurements and measurements of amplitude of the emission. This approach is possible in both, the time domain and the frequency domain.

In the time domain the sample is excited with short light pulses and its emission fluorescence is monitored as a function of time after excitation by each flash of light.

According to the signal processing theory, this is equivalent in the frequency domain to excite a sample with a wave-type excitation [25].

This method is called frequency domain emission spectroscopy. This one, the frequency domain approach, was chosen to evaluate the new spectroscopic techniques that are described throughout the work.

2.1.1 Frequency domain measurements

As it is aforementioned, a method of exciting samples in spectroscopy in order to obtain time resolved measurements, is about exciting them with short flashes of light or either with light whose intensity is modulated.

Within the time formalism, the relaxation of the emission of the sample can be described in this way:

$$f(t) = f_0 e^{\frac{-t}{\tau}} \qquad (1)$$

And its Fourier transform can be easily obtained:

$$F(\omega) = f_0 \int_0^{\infty} e^{\frac{-t}{\tau} + i\omega t}\, dt = f_0 \cdot \frac{1}{\frac{1}{\tau} - i\omega} \qquad (2)$$

In the same way that the relaxation of the emission can be described in either one of the two domains, it is possible to obtain a response from the sample already in the frequency domain, by exciting it with a sinusoidal function instead of a pulse.

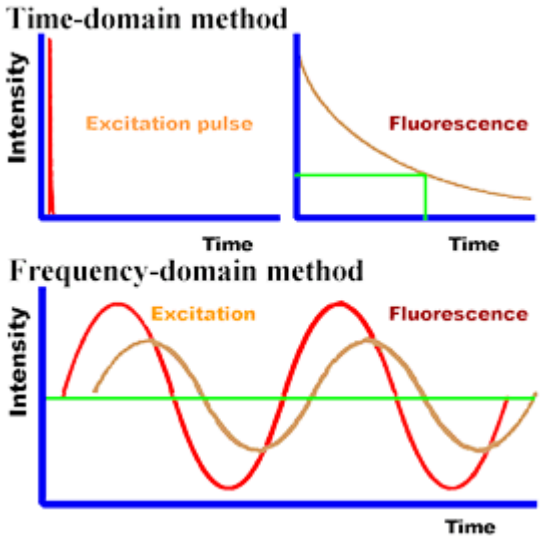

Fig. 8: Time domain vs. Frequency domain [26].

When this is done, the sample emits light directly following the excitation, at that same frequency but with a certain demodulation and time delay measured as a phase angle, as showed in the following figure:

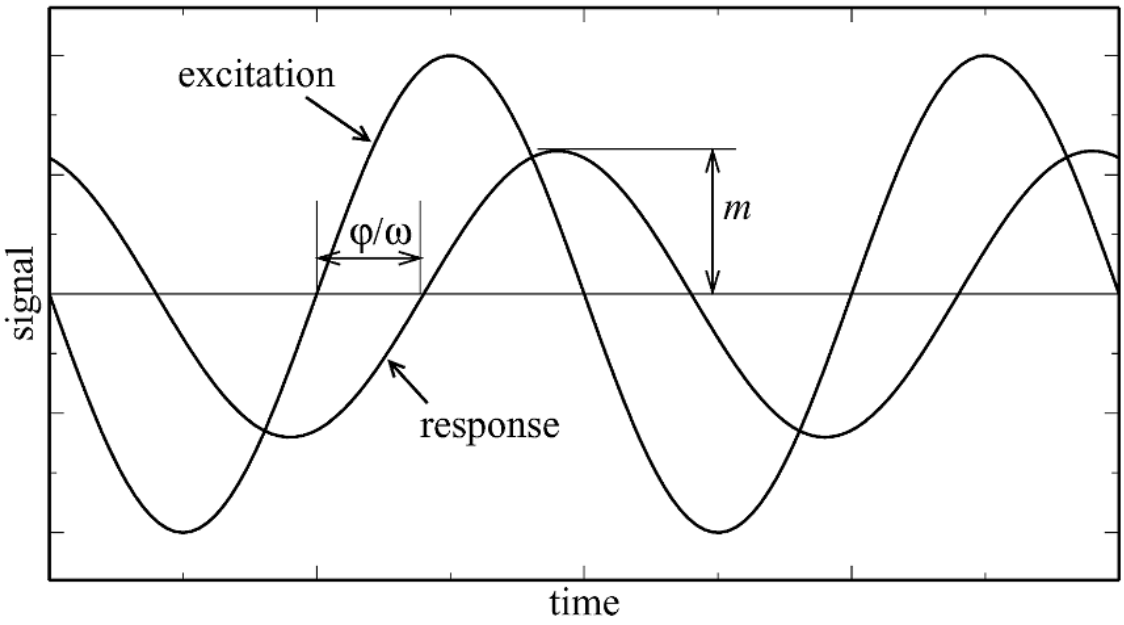

Fig. 9: Excitation and response signals [25].

The frequency response has the following form:

$$r(t) = F_{Re}(\omega)\cos\omega t + F_{Im}(\omega)\sin\omega t \qquad (3)$$

Were the amplitudes of the sine and cosine are the real and imaginary parts of $F(\omega)$:

$$F_{Im}(\omega) = Im(F(\omega)) = f_0 \cdot \frac{\omega\tau^2}{(\omega\tau)^2 + 1} \qquad (4)$$

The amplitude of the sample response, can be obtained as the modulus of the response function.
At the same time, its delay relative to the excitation can be obtained as the phase of the response function:

$$m = \sqrt{F^2{}_{Re}(\omega) + F^2{}_{Im}(\omega)} \qquad (5)$$

$$\varphi = \tan^{-1}\frac{F_{Im}}{F_{Re}} \qquad (6)$$

This expressions, for exponentially decaying emissions, become the following ones:

$$m = f_0 \frac{\tau}{\sqrt{1 + (\omega\tau)^2}} \qquad (7)$$

$$\varphi = \tan^{-1}(\omega\tau) \qquad (8)$$

The first one, describes the amplitude that is demodulated with respect to the one of excitation, as it is explained before.

The demodulation of the emission happens because the finite lifetime of the excited state prevents the emission from precisely following the excitation, sometimes making both signals to interfere.

The second expression describes the delay of the emission relative to the light modulation. This delay is produced by the time that passes from the moment when light absorption takes place until the moment when light emission occurs.

The demodulation and the delay are only present when some kind of fluorescence is being emitted and that is not only the reflected light from the sample's surface what is being detected.

The phase shift and the peak-to-peak intensity of the modulated emission are useful to extract the fluorescence lifetime information.

If a sample is excited with light modulated with a different frequency each time and every time measurements of phase and amplitude are taken, two exponentials, one from the phase and one from the amplitude, are obtained when the respective measurements are plotted versus frequency.

As the frequency of modulation increases, the amplitude of the emission decreases and the phase angle of delay increases; therefore obtaining a decaying exponential curve from the former data and an increasing exponential curve from the later one.

This exponential curves describe the form of the sample's intensity decay law, which further on, can be fitted to determine sample's lifetime.

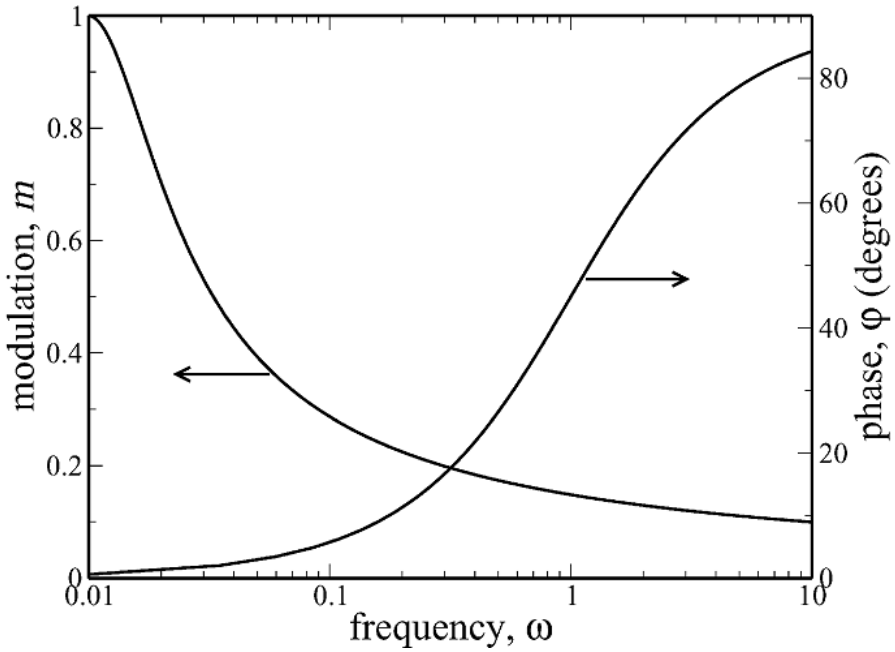

Fig. 10: Modulation and phase curves [25].

One thing that has to be taken into account in order to obtain the decay is to work in the useful range of frequencies over which it is possible appreciate the fluorescence phenomena, this is where the increasing phase delay and the decreasing intensity exponential curves.

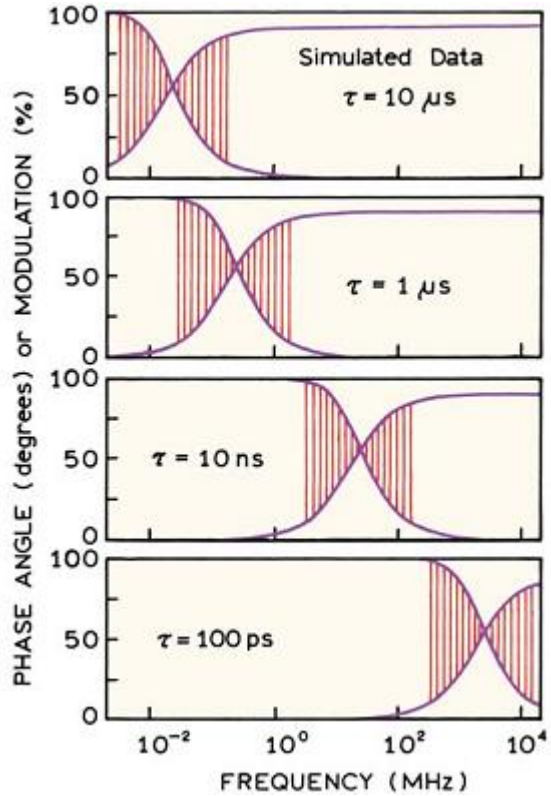

Fig. 11: The useful range of frequencies is related with the lifetime of the sample [22].

Once that the useful range is identified, this measurements are taken making a frequency sweep over this range in order to calculate the lifetime later on.

2.1.1.1 Synchronous detection

The detection of the fluorescence measurements is carried out by a method called synchronous detection.

Synchronous detection is a type of signal recovery approach, since the type of fluorescence signals that are aimed to be detected are very small in comparison with other possible noise sources in the surroundings.

It works with the principle that the emission of fluorescence always conserves the same frequency of excitation but reflectance and other noise sources may not.

The instrument in the core of synchronous detection is a lock-in amplifier, to which a reference signal is usually introduced.

This reference is the signal of excitation that has the desired frequency of reference. The lock-in singles out just the component of the detected signal at that specific frequency, which is fluorescence.

In this way, all other signals at a different frequency than the reference one are rejected and just measurements from the signal that is wished to be detected are retrieved.

The way this is done in the lock-in amplifier is first, by amplifying the detected signal. Then, the reference sine wave is multiplied by the detected signal which is composed of many harmonics. If the reference signal and one of the harmonics are multiplied, two AC signals are obtained [27].

$$V_{Response} = V_{sig} \sin(\omega_r t + \theta_{sig})$$

$$V_{Reference} = V_L \sin(\omega_L t + \theta_{ref})$$

$$V_{PSD} = V_{sig} V_L \sin(\omega_r t + \theta_{sig}) \sin(\omega_L t + \theta_{ref}) =$$
$$= \frac{1}{2} V_{sig} V_L \cos[(\omega_r - \omega_L)t + \theta_{sig} - \theta_{ref}]$$
$$- \frac{1}{2} V_{sig} V_L \cos[(\omega_r + \omega_L)t + \theta_{sig} - \theta_{ref}]$$

If the signal resulting from the product with the two AC components is passed through a low pass filter, both components become negligible.

Signals with a higher frequency $(\omega_r - \omega_L)$ are attenuated the most. Only for the case on which the subtraction of both frequencies is equal to zero $(\omega_r = \omega_L)$ the signal has a DC component that is not attenuated by the low-pass filter. Only this part of the signal remains.

This permits the elimination of noise content in the signal at frequencies far from the reference one, which will not be close to DC. Only noise at frequencies very close to the reference frequency will result in very low frequency AC outputs.

In mathematical terms, the operation of the multiplier followed by the low pass filter is equivalent to multiply two orthogonal functions which can be two sine waves that differ in frequency, so the average of the product is always zero unless the frequencies are exactly the same.

Hence, ideally what is retrieve by the lock-in is just the signal of interest but what is recovered is principally the signal of interest and very little noise, since it has decreased a couple of orders of magnitude.

The lock-in displays the intensity of the singled out component and the phase in degrees between the detected and the reference signal, at a specific frequency. Further on, this measurements can be interpreted and processed to provide information about the sample.

2.2. Application of the theoretical framework to the problem of the cell count

2.2.1. Introductory approach to a previous problem

By obtaining the fluorescence measurements of a sample, there are more features that are possible to be determined, and these ones may be practical for the development of applications, as it is for the developed problem that is going to be described in this part of the work.

It was found very helpful to follow the course of this experiment and the development of the described application in order to have a reference on the methodology of working.

This application consists on the build of a remote optical sensor for the detection of the presence of salt on road surfaces, to determine which concentration of salt was applied [28].

The determination of the salt concentration on road surfaces is useful to know if it is sufficient to accomplish anti-icing and at the same time, is not harmful to motor vehicles nor to the environment.

The sensor provides real-time measurements of the amplitude of fluorescence and decay time allowing to detect concentrations of salt as small as 20 g/m^2.

This is possible because Sodium Chloride natural fluorescence, as theory explains, has a strong dependence on frequency in a low frequency range, so both decaying curves (amplitude and phase) could be detected within this range by modulation of the light of excitation.

In this experiment, three different types of salt were considered and were analyzed under a fluorimeter, which revealed that the three of them shared an excitation peak and two absorption peaks.

In this way, the salt is excited by using an emitter with the wavelength of excitation shared among the three and the emission is collected with a receiver at one of the two emission wavelengths found. The receiver is composed of and optical sensor and a pass-band filter connected to the lock-in amplifier.

The light of excitation is in this case, is modulated by the own signal generator of the lock-in.

The signal, detected by synchronous detection, is further imputed to a signal processing system.

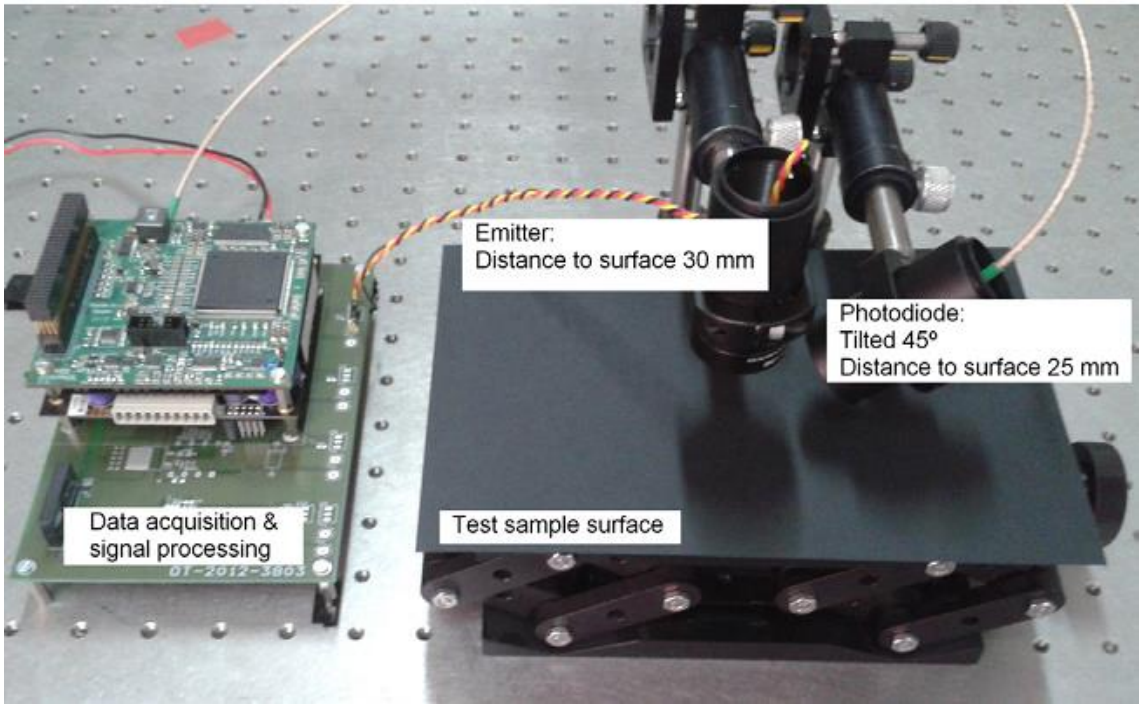

Fig. 12: Complete system for the remote optical sensor [28].

In the experiment it was possible to obtain both exponential curves in a range of 4 Hz to 1 kHz. The data presented in the curves was fitted in order to obtain the lifetime of the sample.

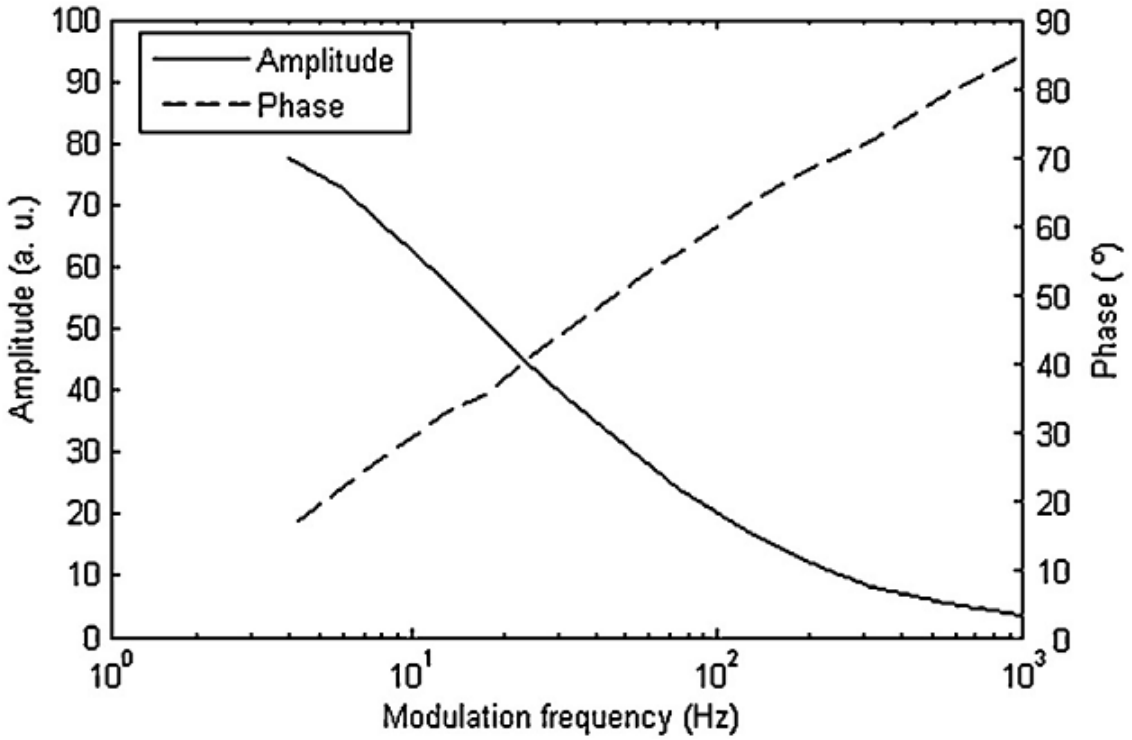

Fig. 13: Data of amplitude and phase [28].

Knowing the lifetime of a sample is important at the time of determining the optimal frequency of excitation, which is close to the inverse of the sample lifetime.

At this frequency, the maximum amplitude of fluorescence is being obtained and at the same time is being ensured that is fluorescence what is being detected and not reflectance of the light at the surface.

This optimal frequency is used to modulate the light of the LED to excite the subsequent concentrations of salt. Finally, a relationship between the amplitude of fluorescence at each given concentration of salt in the samples is found.

2.2.1. Adaptation to the problem of cell counting

These approach for the determination of salt concentration in road surfaces, can be extrapolated to the problem of the determination of cellular concentration.

In this case the samples, cultures of cells at different concentrations, are also illuminated with a frequency modulated light, in order to be able to detect the signal emitted by the sample at that same frequency.

The component of the signal that corresponds to fluorescence preserves the same frequency of the light of excitation, as explained above in the theory. In this case, the samples were not excited in the range of frequencies where the phenomena of demodulation and phase shift are obtained, but in a range of frequencies way smaller, being able to obtain just the amplitude function.

The range of frequencies where these phenomena are present is way above, in the range of MHz, and it was not possible to detect in such a high range of frequencies with the equipment used. So the lifetime of the sample, obtained by the fitting of time resolved measurements in the introductory problem, is not obtained in this case.

But the measures of amplitudes in between 1 kHz and 100 kHz are enough to find a relationship with the number of fluorophores present in the sample.

The number of fluorophores are proportional to the concentration of cells in the area of illumination which are proportional to the fluorescence intensity measured.

2.3. Application of the theoretical framework to the detection of glucose-related AEGs' fluorescence

Blood plasma samples with different glucose concentrations are also excited with a frequency modulated light to be able to detect its amplitude of fluorescence by synchronous detection.

But in this case, the data obtained to distinguish among different glucose concentrations are ratios of the different amplitudes of emission obtained at different wavelengths.

The theory for the development of the glucose study was obtained from a previous approach to the measurement of glucose levels in blood plasma.

2.3.1. Previous problem for the basis of AEGs' fluorescence detection

In this experiment, the authors found a relationship between the native fluorescence of blood plasma and its content of glucose by means of fluorescence spectroscopy [21].

This study had the purpose of better understanding which elements of blood plasma could be associated to the content of glucose in blood.

One process associated to the formation of glucose is the nonenzymatic glycation of proteins in blood. It is known that if glucose in blood increases abnormally, it leads to an accelerated glycation of proteins, and the formation of advanced glycation end-protucts or AEGs.

These end-products are known to have a native strong fluorescence, but its fluorescence needed to be related to the glucose content in blood.

To be able to demonstrate this relationship, the kinetics of nonenzymatic glycation of albumin are studied in this experiment.

In the laboratory, albumin is incubated with glucose and after 20 days its fluorescence was found to be 10-fold greater than normal, therefore relating the AGE-related fluorescence with the presence of hyperglycemia.

Afterwards, it is studied which can be the best excitation wavelength in order to make a distinction among the spectrum of emission of the group with a high content in glucose and the one with a normal one.

The samples of blood plasma are obtained from a control group of rats and another one with hyperglycemia.

The study revealed that the spectra of both types of samples showed a major difference at an excitation wavelength of 320 nm.

With this wavelength of excitation the spectral band shape is different for the two groups and this difference can be characterized as it is showed in the following figure, by making the ratio of the intensities at 390 nm and also at 450 nm.

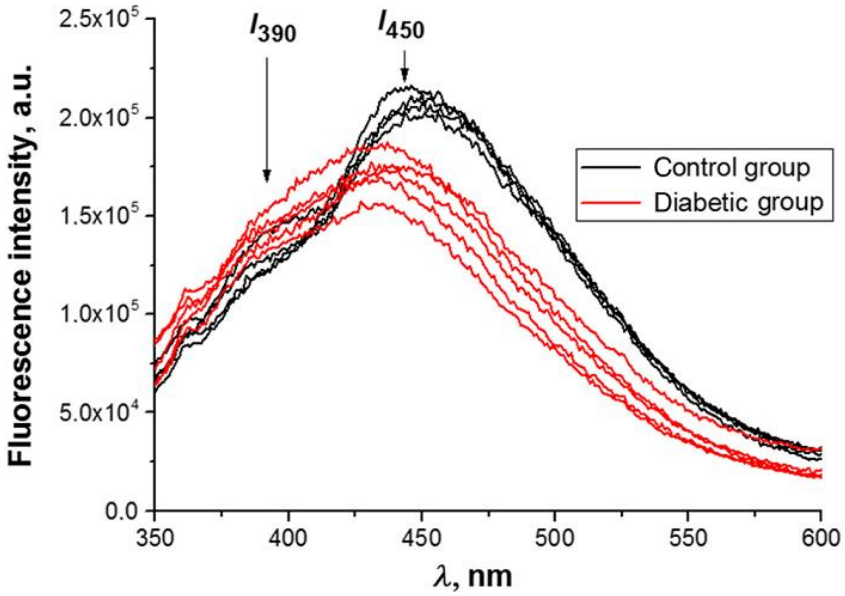

Fig. 14: Fluorescence spectra of the diabetic and the control group [21].

The intensities at those points vary almost 1.5 times from one group to another.

But with the purpose of making a deeper analysis of the fluorescence spectra, they made a deconvolution of both of them into three Gaussian peaks as it is showed in Fig. 15:

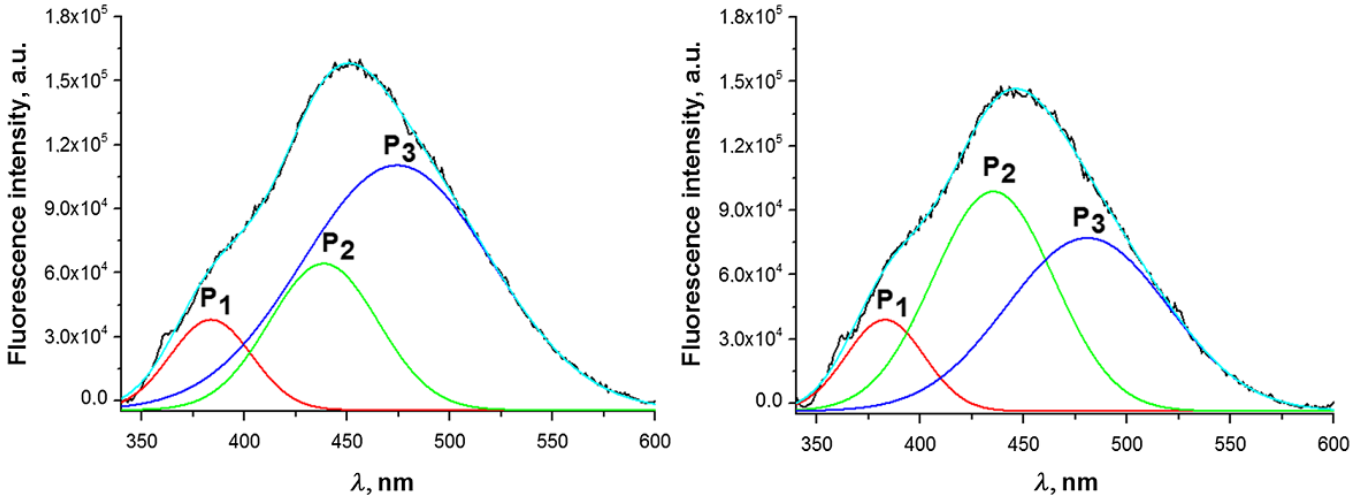

Fig. 15: Decomposition of the fluorescence spectra [21].

It was found that the first Gaussian peak is constant between the two groups and is attributed to other source of fluorescence, tryptophan residues, which produce the intrinsic fluorescence of proteins.

The two other peaks, P_2 and P_3, are different among the two groups and are the analogues of the intensity peaks found at 390 nm and 450 nm in Fig X and hence, can be attributed to the fluorescence of AEGs.

The difference between the ratio P_2/P_3 among the diabetic group and the control one, permitted to make a relationship between the value of this ratio and the glucose content in blood plasma.

The results that the authors obtained show that the ratio P_2/P_3 in the diabetic subjects is significantly higher than the one in the control subjects.

2.3.2. Adaptation of the previous problem to detect glucose-related AEGs' fluorescence

In order to approach glucose detection in this work, similar blood plasma samples are obtained, which can be separated into two groups, samples from prediabetic animals and samples from diabetic animals.

But in this case, instead of using a fluorometer to analyze the spectra and its decomposition, the emission amplitude is directly detected with the system at the three different wavelengths, were the three Gaussian peaks were found to be centered in the bibliography.

This is done by means of filtration of the emission light with three different band pass filters at the beginning of the synchronous detection system.
This simplifies a lot the method for sorting the samples into healthy or diabetic and in addition, the system is way more affordable than a fluorometer.

Fluorescence amplitudes are obtained at the three wavelengths and the ratios between the three of them are obtained. This ratios are compared among one group and the other one in order to look for a sorting criteria of the samples.

3. Description of the instrument

Along this chapter, the optical principles, the equipment and the electronic and optical instrumentation required for assembling the instrument required in each evaluation are explained as well as the proposal of different alternatives and methodology.

The instrument is composed of a common system for each kind of sample, which includes a light emitter to induce fluorescence and an optical receiver to detect it.

Then, according to the specific spectrums of absorption and emission of the samples and the methodology of each experiment; optical setups, light wavelengths of excitation and filters within the emitter and the receiver are changed on each case.

In this section it is described the complete instrument and the particular setups for the analysis of each sample.

3.1. Instrumentation for the modulation of light and detection of fluorescence

The instrumentation involved in the modulation of the light of excitation and in the detection of the emitted fluorescence is the common system used on each experiment.

The emitter is composed by a LED controlled by a laser diode driver modified to bias the LED in order to protect it from surpassing the limits of current and voltage on its specifications and to which the sinusoidal signal generated by a signal generator is supplied.

Three different possibilities were tried in the system to find out which one was producing the most optimal response of the LED.

The first one, was the connection of a commercial laser diode driver ITC 510. The second one was the connection of an LDD P1 laser diode driver with a commercial circuit to the system. The third one was the connection the LDD P1 laser diode driver to the circuit in the salt monitoring sensor.

The three of them were tested, and based on the highest detected intensity of the LED emission, the commercial driver was chosen for the assessments in this work.

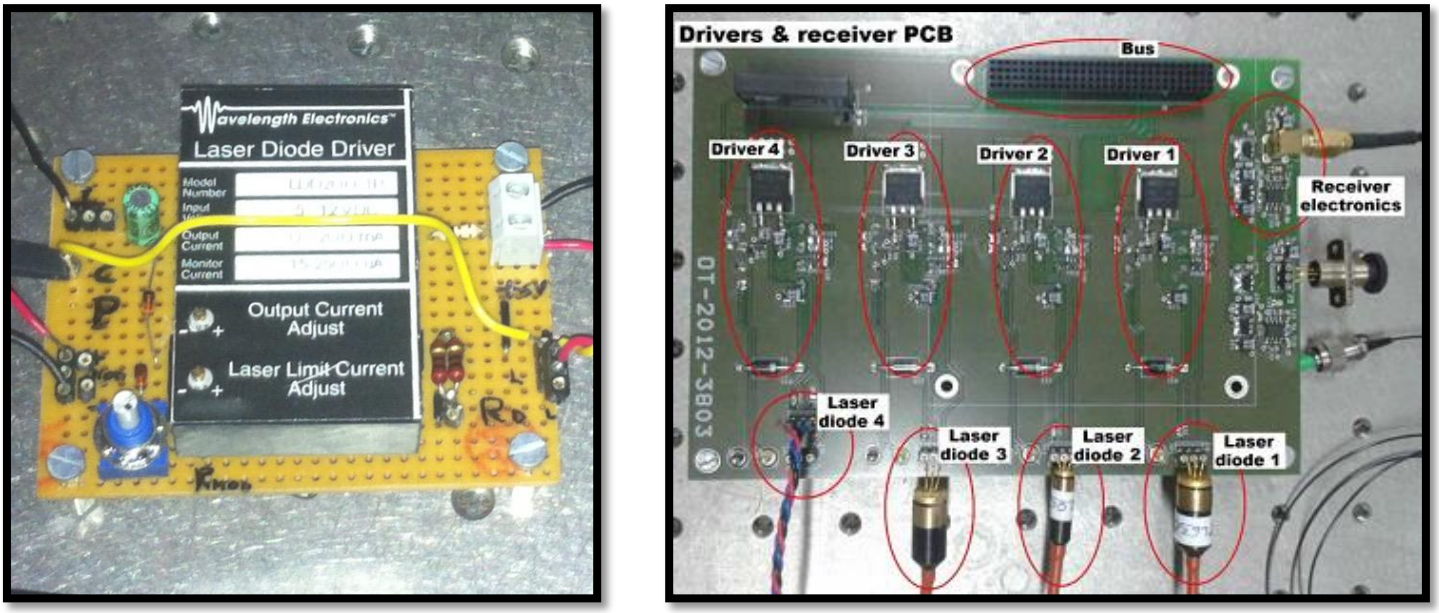

Fig. 16: Circuits for the connection of the driver LDD P1 [29].

In the detection of the fluorescence signal, a low cost silicon detector is used as the head of the receiver. It is connected to the input of a lock-in amplifier to approach the detection of fluorescence by synchronous detection.

The lock-in amplifier is supplied with the same sinusoidal signal generated to modulate the LED as a reference signal, so it is able to select the just the fluorescence coming from the sample that is emitted with that same frequency. It is sensitive to the variations between the two signals introduced, as it was explained already.

The model used was Stanford Research Systems SR830.

Fig. 17: Lock-in amplifier [30].

The lock-in is also able to generate a signal of reference and use this one to modulate the emitter, but as it is reported in the bibliography, this may cause some phase and amplitude distortions.

Nevertheless, in the first approach to the detection of fluorescence, also the lock-in generator was used to modulate the emitter.

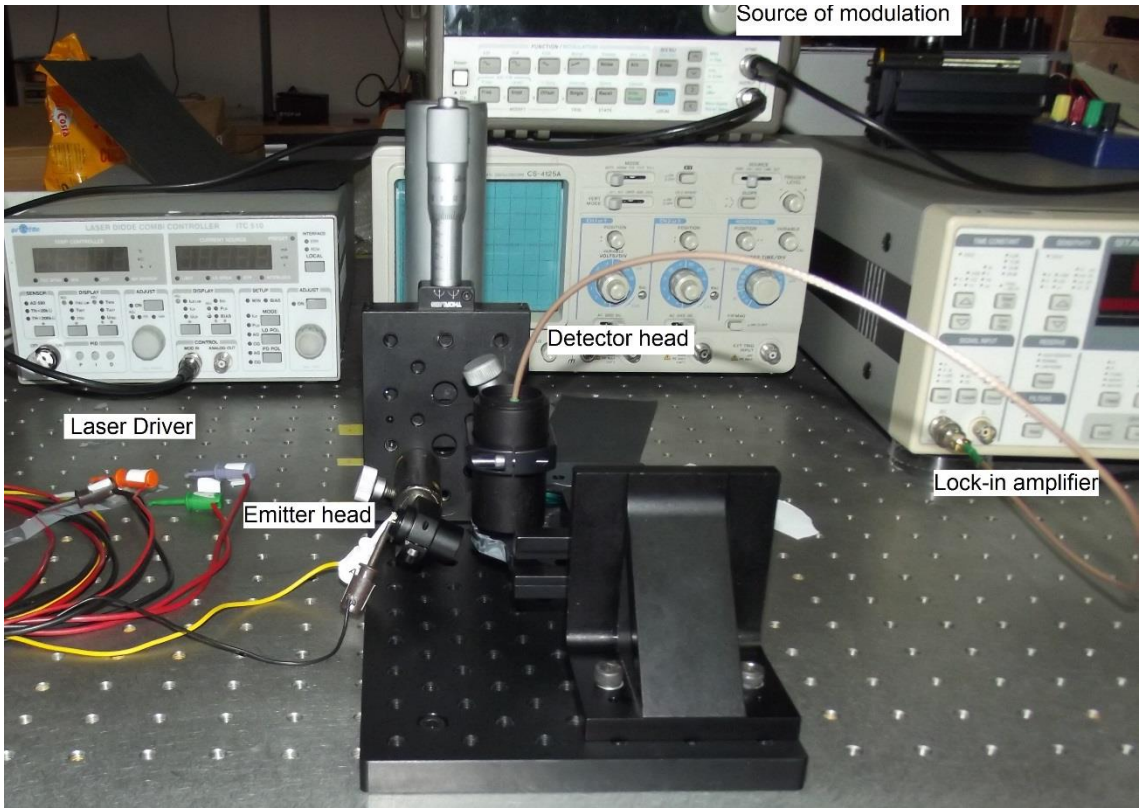

Fig. 18: Overview of the system.

This is the experimental equipment for the measurement of fluorescence, but this whole system could be reduced to a small instrument where the lock-in amplifier is substituted by a FPGA and all the instruments involved in the modulation by an equivalent electronic power supply.

Hence, a cheap and compact equivalent system is possible to be further assembled.

3.2. General optical setup for the measurement fluorescence

The optical setup for the collection of the samples fluorescence is similar among all the studies and has some common parts.

The example of the salt fluorescence detection served as an example in order to familiarize with the optics involved and their arrangement in the prototype to detect fluorescence.

Optics

All optical setups are composed of an emitter head and a detector head, as explained a few paragraphs above.

The emitter head is an optical mount into which the corresponding LED is screwed. This tube limits the area that the LED illuminates to a circular spot of 60 mm.

The LED is chosen according to its wavelength of emission, for it to be as close as possible to the wavelength of excitation of each sample.

In order to achieve the closest similarity among the LED's emission spectra and the ideal spectra of excitation, a band pass filter is also screwed into the front of the mount tube, in between the LED and the sample.

By the side of the emitter head and close to the sample, the receiver head is assembled and fixed.

The emitter head is also a mount tube into which a silicon detector model Thorlabs FDS100 with an active area of 13 mm^2 is screwed. There is also a band-pass filter into the front part of the tube, in order to select the wavelength that is wished to be detected. The band-pass filter is chosen to select the wavelength of the emission spectra peak and avoid the detection at other wavelengths different from this one.

It has to be taken into consideration at the time of choosing both band-pass filters that the spectra of excitation (produced by the emitter head) and the spectra of excitation (detected by the receiver head) have to be as separated from each other as possible.

The band-pass filters chosen on each case were found to be optimal to narrow both spectra around the desired wavelengths and separate the spectra as much as possible from each other.

Mechanics

The emitter and the detector heads are arranged around the sample for its best illumination and detection of the fluorescence. For this purpose, the illuminated surface in the sample is made to coincide with the field of view of the detector.

But it needs to be taken into account that the conditions of best illumination and measurement collection will be achieved with the emitter head and the detector head as close as possible to the sample.

Also, although band-pass filters are included in the system, it is good to arrange both heads as close as possible to each other in order to avoid direct illumination to the detector.

In order to follow this considerations, both heads are placed the closest to the sample and the closest to each other that the coincidence of the illuminated area with the detector's field of view permits.

The way of arrangement to do so is achieved by placing the head of the emitter in the mount tube vertical to the surface of the sample and the receptor head making an angle of approximately of 45º with respect to the vertical plane.

The heads are fastened in posts and these ones are screwed to optical panels, in order to fix the optical setup of the prototype around the sample. Is important that the heads remain in the same place and height during all the measurements in order for the results to not be affected.

The tube mounts, as well as the posts and the holders could be designed for the specific requirements of each study and 3D-printed. This possibility also offers a big decrease in the costs of the optical assembly, because usually this kind of optical components are expensive.

If 3D-printed versions are well-designed, they can resemble very much and accomplish the same functions as the real optical components.

When the salt experiment was repeated in order to check on the good functioning of the common system for the following analyses, it was decided to replace the restraint system that held the optics by a 3D-printed holder.

The holder was designed to further improve the functionality of the system's mechanics. This holder permits to change the arrangement of the heads in the easiest and most practical way.

This is a T-shaped holder, showed in the following figures, with two circular holes to fit in two cylindrical bars. Both bars have a hollow type holder at the tip to grip the mount tubes.

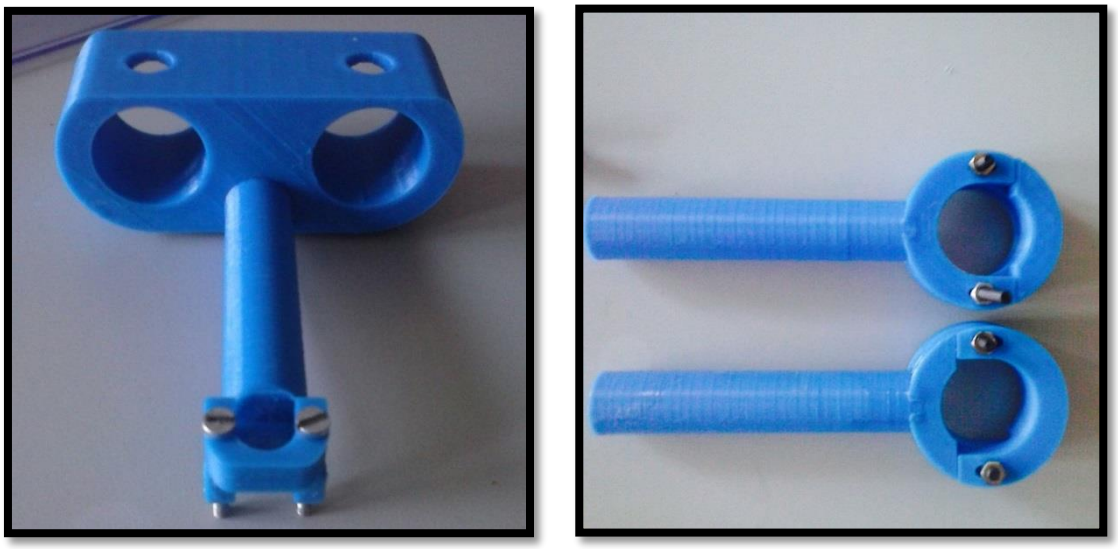

Fig. 19: 3D-printed optical mount.

In the large harm of the T-shaped holder there is also a hollow type grip to hold on the ’T’ with both heads to a vertical bar at a certain height.

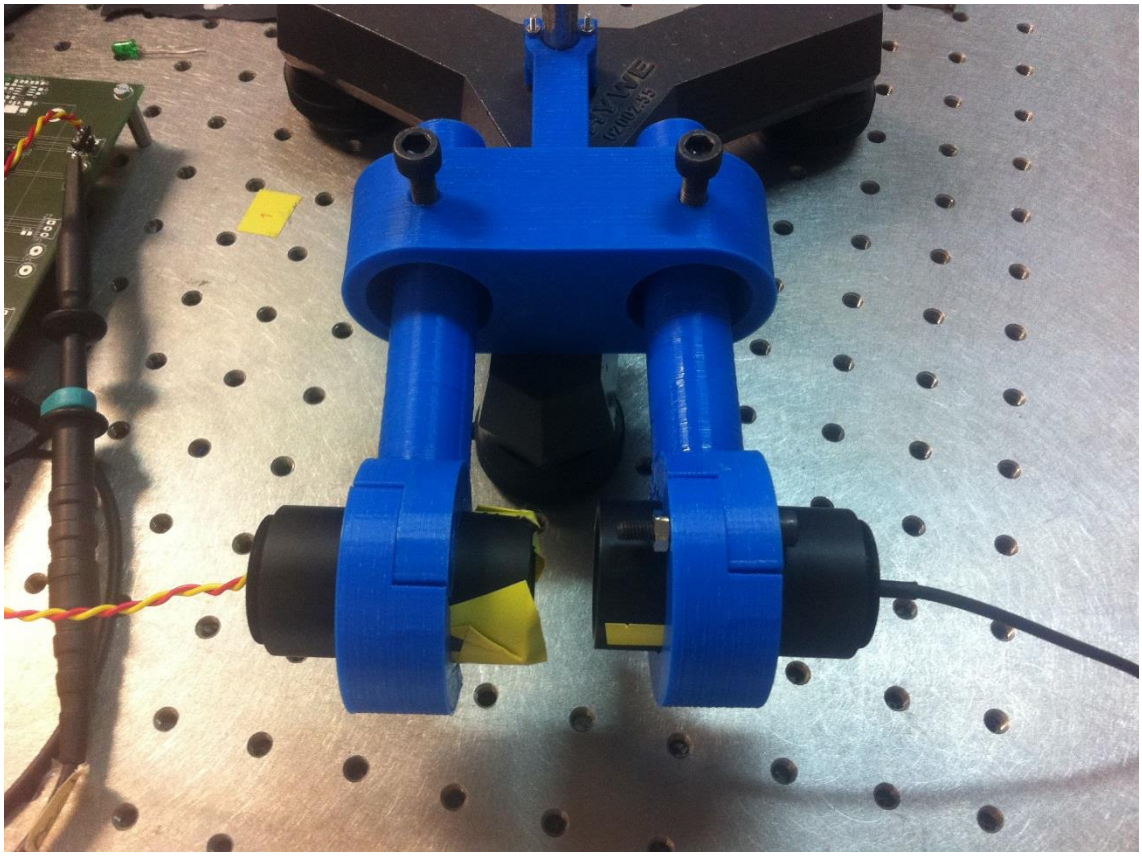

Fig. 20: Overview of the 3D-printed optical mount.

The only disadvantage of the design of this holder was that the proximity to which both heads could be placed was limited by the width of the holder.

This holder is 3D-printed and is a proof of how all optical mounts and holders of the instrument could be obtained this way, instead of purchasing them.
Optical mounts and holders for optics are usually quite expensive and 3D-printed versions are the same robust.

The design of this proposed optical holder was carried out with Solid Edge and OpenScad. The pieces were printed with a 3D printer model Power Code using Cura and Pronterface as the programs to load the model for printing.

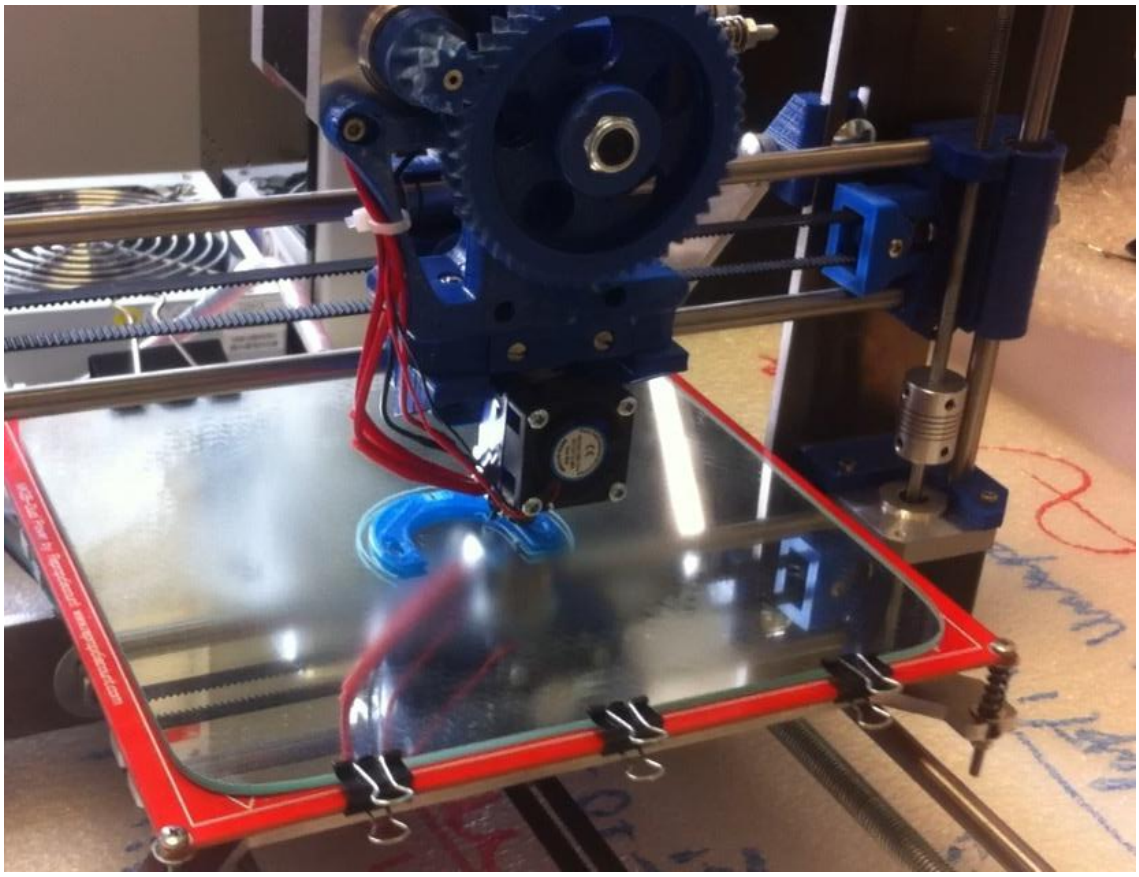

Fig. 21: One of the pieces of the holder being printed.

The printing material used was ABS plastic, which is a very resistant material but also easy to sand for a better coupling of pieces.

This type of plastic is easily dissolved with acetone and dries very quickly, so the pieces of the holder that had to be printed separately, were easily assembled by moistening the surfaces to be glued with acetone and letting them dry together.

Once the system with the instrumentation for light modulation, optical setup and synchronous detection is fully installed, the detection of the fluorescence of a sample is ready to be tested.

3.2.1. Optical setup for the measurement of cellular concentration

The optical setup for the analysis of the cell samples is very similar to the one described in the experiment of the salt.

The excitation and emission wavelengths differ from the ones in the salt experiment. In this case the aim is to excite HaCaT cells infected with a retrovirus that contains the sequence of the fluorophore green fluorescent protein or GFP. A retrovirus is a virus containing a single strand of RNA which is translated into DNA and inserted into a host cell at the time of infection; in this case the DNA information to be expressed is the one of the GFP.

The GFP is a fluorophore that emits green light when ultraviolet light is shined upon the cells.

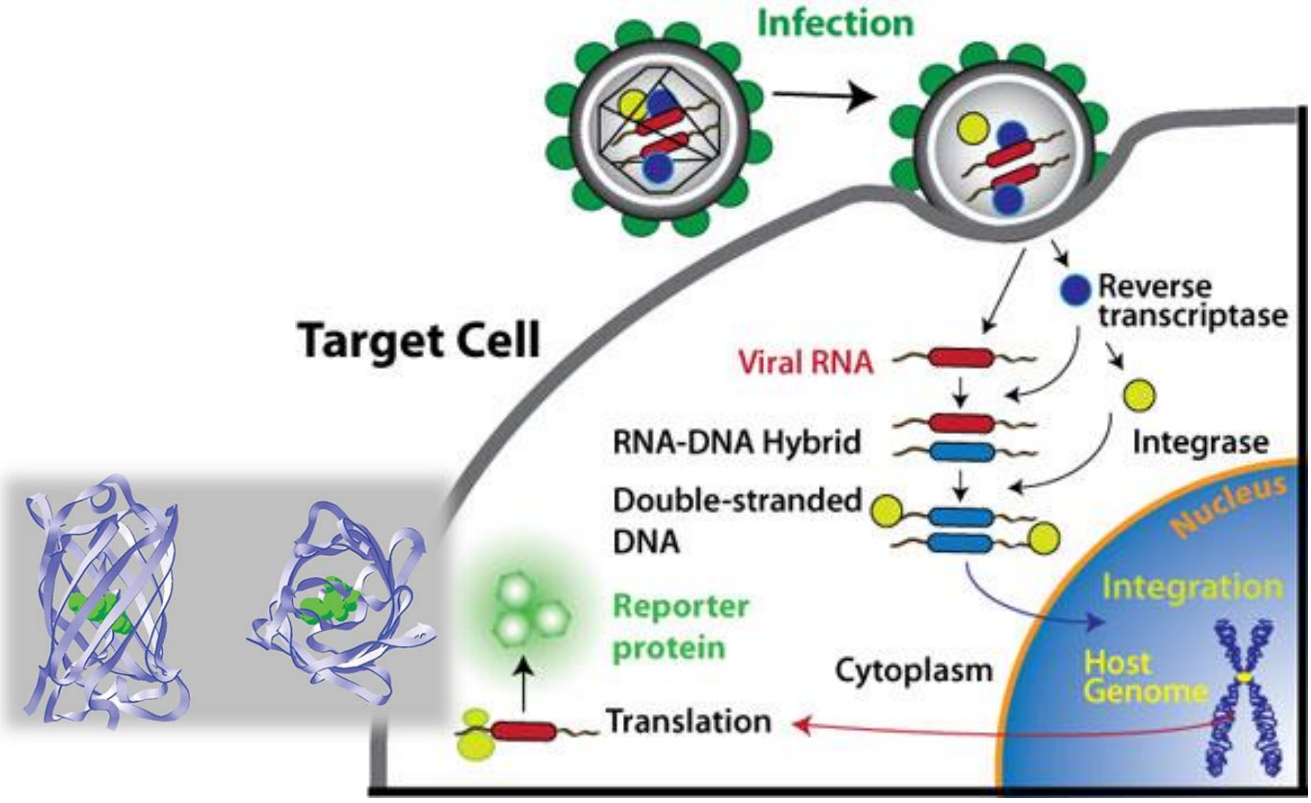

Fig. 22: Schematic representation on how a retrovirus containing the GFP genetic information infects a cell [22, 31].

This makes possible the visualization of the cells under a fluorescence microscope and also, if wished so, the visualization of specific structures of the cell to which GFP is specially targeted.

It is also possible to detect the fluorescence coming from the cells or coming from some inner structures with a system of spectroscopy.

Optics

There exists different variants of GFP with different excitation and emission peaks. The GFP used had a major excitation peak in blue, at 488 nm and an emission peak at 509 nm (green).

For this purpose, the LED chosen to be installed on the emitting head is model Roithner LaserTechnik LED490-06 and emits with a wavelength of 490 nm. The receiver head is as well prepared to detect a wavelength in the green of 509 nm; for this purpose, a band pass filter is placed before the silicon detector model Thorlabs FB520-10 with a FWHM of 10 ± 2 nm around a wavelength of 520 ± 2 nm.

In order to concentrate the spectra of the LED around the required excitation wavelength, also a filter model FL05488-10 is placed after the LED. This filter has a FWHM of 10 ± 2 nm around a wavelength of 488 ± 2 nm.

A threaded mount is used to couple the LED to the filter into a tube mount. The tube mount is held in a slip ring.

The use of the band-pass filters is very important in order to correctly separate the spectra of excitation from the one of emission.

Also a convergent lens of focal distance f = 40 mm was placed in front of the LED in order to eliminate the motif that the illumination of the LED makes on the sample, in order for it to fall upon the sample homogeneously.

Mechanics

Both heads are placed around the sample in a way that the light of the emitter loses as less power as possible in reaching its surface and so does the light of emission in reaching the receiver. In addition, of course, they are arranged in a way that permits the detector to collect all the light in the field of view of illumination.

The emitter and receiver heads, as in the case of the salt, were arranged to be as close as possible to the Petri dish containing the culture.

The complete optical system and excitation of the sample is showed in the following figure Fig. 23:

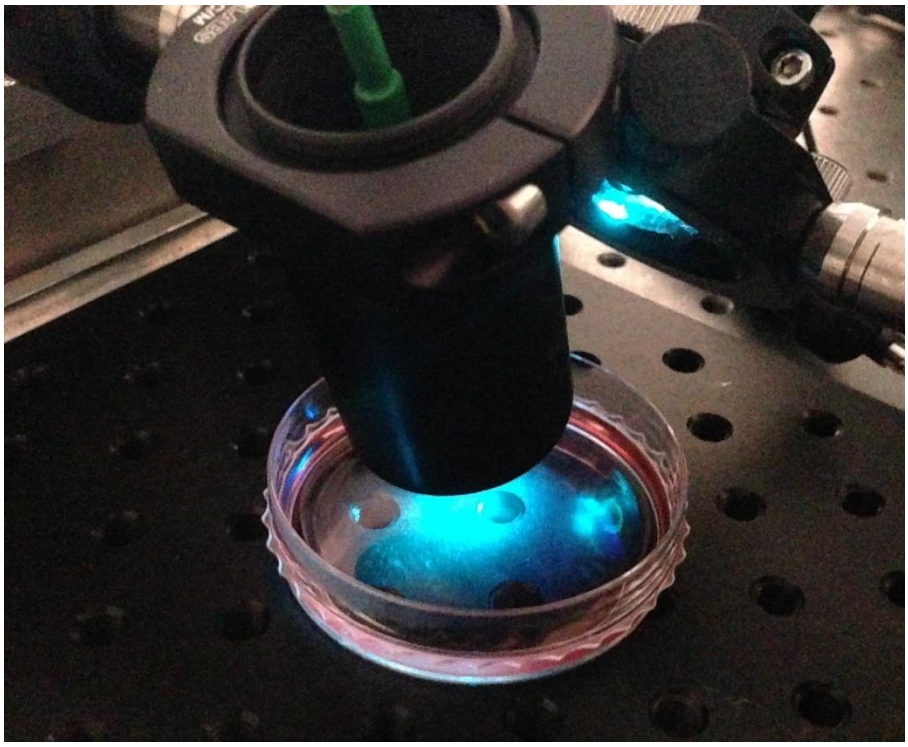

Fig. 23

3.2.2. Optical setup for the measurement of AEGs' fluorescence

The optical set-up used in this case is somewhat different to the ones in the previous cases. The system is modified in order to obtain measurements of amplitudes at three different wavelengths.

As explained in the previous chapters, embedded in blood plasma there are some glycation end-products. This products called AEGs arise from the advanced non enzymatic glycation of plasma proteins and provide a powerful source of fluorescence. From the bibliography, it is known that this source of fluorescence can change, depending on the amount of glucose.

In addition, due to the residues of tryptophan, blood plasma proteins emit fluorescence themselves, but this fluorescence is thought to be constant in any case.

The fluorescence of this two sources can be found to contribute to the emission spectra at three different wavelengths, by its decomposition into three Gaussians.

The amplitude of the different fluorescence sources are obtained from this decomposition in the bibliography.

In this case, the fluorescence amplitudes of this Gaussians are directly obtained from the system, by the selection of the three wavelengths around which they are centered.

Optics and mechanics

This selection is done with the installation of three different band pass filters before the head of the detection, mounted on a filter wheel station Thorlabs FW1A in order to select the filters in the fastest way.

The filters mounted in the wheel are FB380-10, FB440-10 and FB480-10 by Thorlabs.

The blood plasma sample is pipetted into a micro fluorescence cuvette made of transparent quartz and is illuminated with a LED model UVA325-HL5N at 325 nm. The complete system is represented in the following figure Fig. 24.

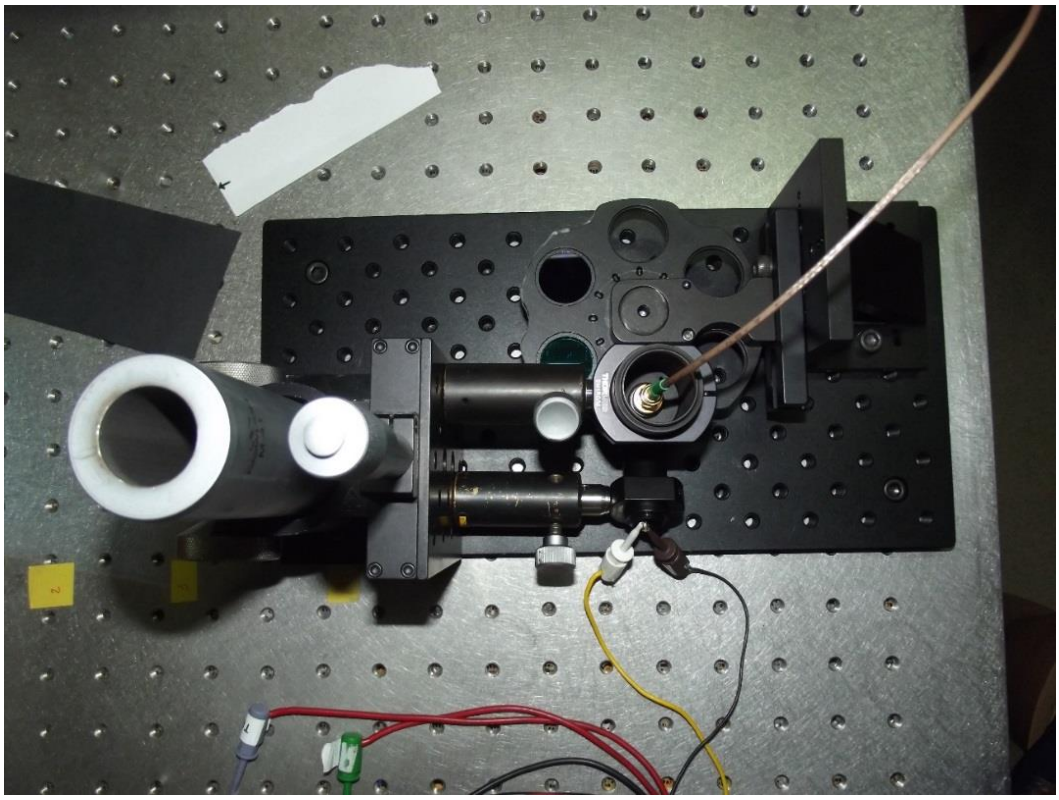

Fig. 24

4. Experimental protocol

Here they are going to be described all the steps involved in the process, from the assembly of the fluorescence spectroscopy instrument until the samples are placed on the table and ready to be analyzed.

All the series of samples and its collection, as well as the interpretation of the data retrieved are described in this section.

4.1. Experimental protocol to measure cell concentration

Instrument assembly

The first step consists on the assembling of the optical setup showed in the following figure:

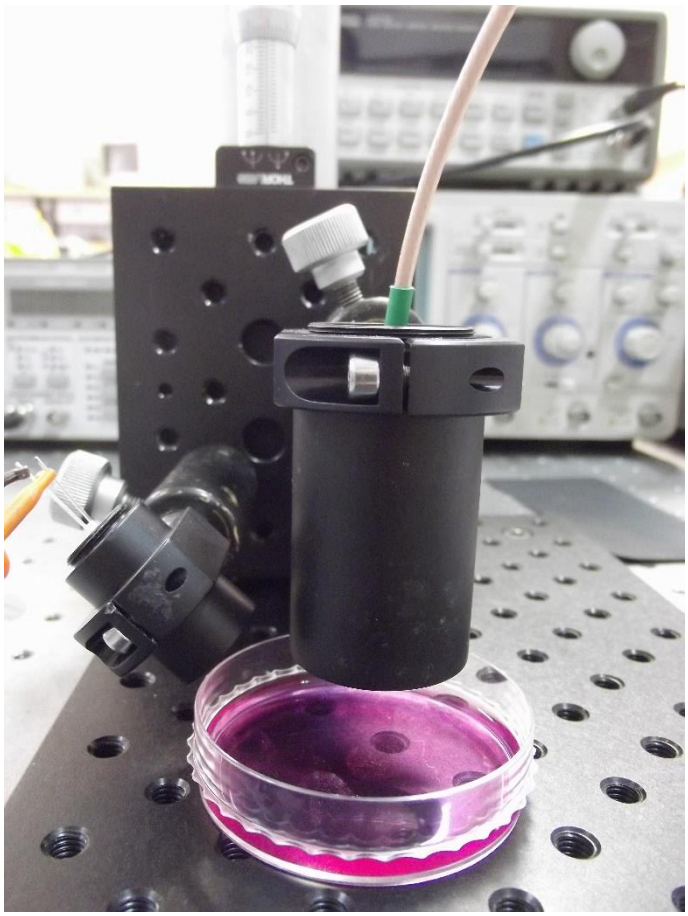

Fig. 25: Optical setup at the beginning

The LED and its filter for the excitation at 488 are placed together on a mount (in the end, an optical lens was also introduced before the LED).
The detector is also placed together with a band pass filter for the collection of the emission at 509 nm.

The common electronic equipment is connected as explained before, for the modulation of the LED and the input of the signal of modulation into the lock-in amplifier.

Cellular seeding and culture

In order to obtain the samples with different concentrations, it is required the cellular seeding and culture of the different cell populations at known concentrations in the cultures laboratory.

The cellular line that was used for this purpose is the well-known HaCaT cell line, which is an immortalized human keratinocyte cell line.

HaCaT cells are utilized for their high capacity to proliferate in vitro. Their use in research allows for the characterization of human keratinocyte. The HaCaT line used was already infected with GFP, as it is explained a few sections above. These cells are kept frozen at cryogenic temperatures in the laboratory of cell cultures.

In order to be able to seed them on a surface for its culture, a thawing protocol has to be followed. The vial containing the frozen cells is removed from the freezer and is thawed either at room temperature or at 37º C in a bath.

It is of a particular importance to sterilize the outside of the vial with plenty of ethanol before opening and handling it.

Afterwards, the cell suspension is transferred to a tube containing 10 ml of complete medium. The volume of the medium must be ten times greater than the one of the cell suspension, which is the volume of aliquote of 1ml with a standard density of 1 million of cells per milliliter.

The tube is then placed on the centrifuge for 5 minutes at 700 rpm at room temperature and the supernatant is discarded. The pellet is resuspended with the appropriate amount of medium and finally, the cells are seeded on a Petri dish type culture surface.

The Petri dish with the cell culture is placed in an incubator at 37 Cº at conditions of 95% of humidity and 5% of CO^2. The cells must remain in the incubator for about 12 hours (one night) to settle and adhere to the plate completely. The next day, they are ready and have increased in number enough to be passed to other culture surfaces at different concentrations for its further analysis.

Once that it is decided to pass the cells at different concentrations, the populations of cells must be analyzed on the morning of the next day after the pass.

This is because the majority of cell lines double their population in between 24 and 48 hours when the conditions in which they remain are adequate; for this reason, in order to conserve the populations of cells with the same known concentrations avoiding its further growth, these must be analyzed on the morning the next day after seeding.

The first step in order to seed the cells at different concentrations is to determine the concentration of cells that is in the culture that was left in the incubator after the thawing and seeding of the frozen cells.

For this purpose, it is used the most common instrument to count cells under the microscope at naked eye, a counting chamber or hemocytometer.

In order to carry out the count, the cells must be resuspended to be loaded into the hemocytometer.

The culture medium is removed and the surface were cells are adhered is properly washed with PBS in order to completely remove the remaining medium. Then, a protease is used, trypsin in order to digest those cellular proteins implied in their attachment to the surface.

The cell culture covered with the trypsin is left in the incubator for 20 minutes in order to obtain the best detachment of the cells avoiding its further damage. Then, some medium is added in order to inactivate the tripsinization process, approximately twice the volume of trypsin.

In order to completely eliminate the trypsin for the best accommodation of the cells in the next passes, the suspension is centrifuged and then the supernatant containing the culture medium plus the trypsin is discarded. Then, new medium is added to the pellet of cells and the cells are again resuspended in the new medium and ready to be counted.

In order to count the average cells over a counting zone of the slide, 5 µl of cell suspension together with 5µl of trypan blue are filled into one of the one counting zone of 10 µl of capacity in the chamber.

The addition of trypan blue has a special importance in the determination of the cellular concentration of this first cell culture, coming directly from the frozen cells, due to properly discard all the cells that died in the thawing process.

Then the chamber is placed under the microscope and the cells are counted by the traditional method at naked eye. Each counting zone has a central grid divided into nine secondary squares, the four ones of the comers divided at the same time into sixteen tertiary squares.

These on the corners are the four quadrants on which the number of alive cells is counted and the average of the four is performed.

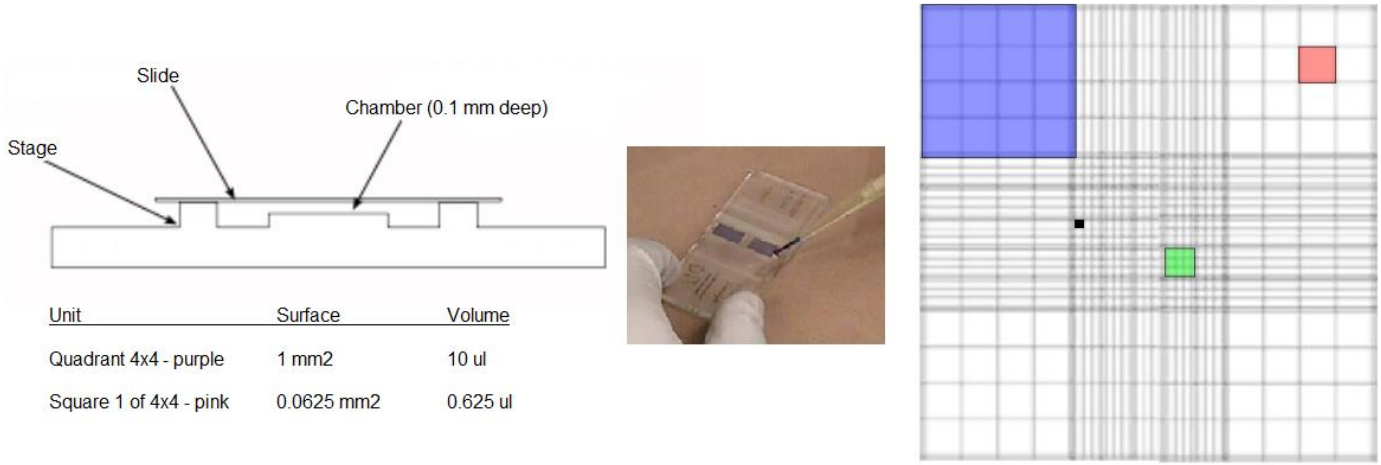

Fig. 26: Hemocytometer and one of its grids seen under the microscope [32].

Then, in order to determine the total concentration in the volume of the cell suspension, the average number of cells is multiplied by two because it was diluted 1:1 with trypan blue and then is multiplied also by the volume of the counting zone, and by the total volume in the suspension of cells [33].

Once it is known the cellular concentration in the first culture we can seed the secondary cultures at different concentrations for its analysis.

For the best analysis and in order to obtain good results, the concentrations of cells that were seeded were different enough in number.

The different concentrations of cells were properly spread over the area of the cell culture surface for them to grow homogeneously.

In all cases, the cells were seeded in the same kind of Petri dish, of 55 mm of diameter and 14 mm of height made of polystyrene and with a capacity of confluence of 3 million of cells approximately.

From one test to another, there was a pass of few cells that was kept in the incubator for the next time it was required to seed cells at different concentrations because all passes that were taken out of the cultures lab to be analyzed were not able to be taken back inside, since outside the conditions of the lab they were contaminated.

The pass that was kept in the incubator had to be maintained by the change of the culture medium once its nutrients were consumed and the cellular waste products were accumulating.

Data collection, measurements analysis and modifications of the system

For the first test with the cells, only two concentrations of one and two million of cells were used, but since the cultures were left on the incubator for too long both samples ended having the same concentrations of cells, which was reflected in the obtained results.

It was observed and has to be taken into account, that the concentrations that have the best chances to grow faster until its analysis are the ones closer to 0.8 million of cells. Hence, there can be some concentrations that don't have exactly the same number of cells as they had when they were seeded.

But the following concentrations chosen are different enough to maintain a clear distinction. For the following tests, five different concentrations of $2.5 \cdot 10^5$, $3 \cdot 10^5$, $5 \cdot 10^5$, $1 \cdot 10^6$, and $2 \cdot 10^6$ of cells were seeded (and were left for a shorter time in the incubator to avoid the problem aforementioned).

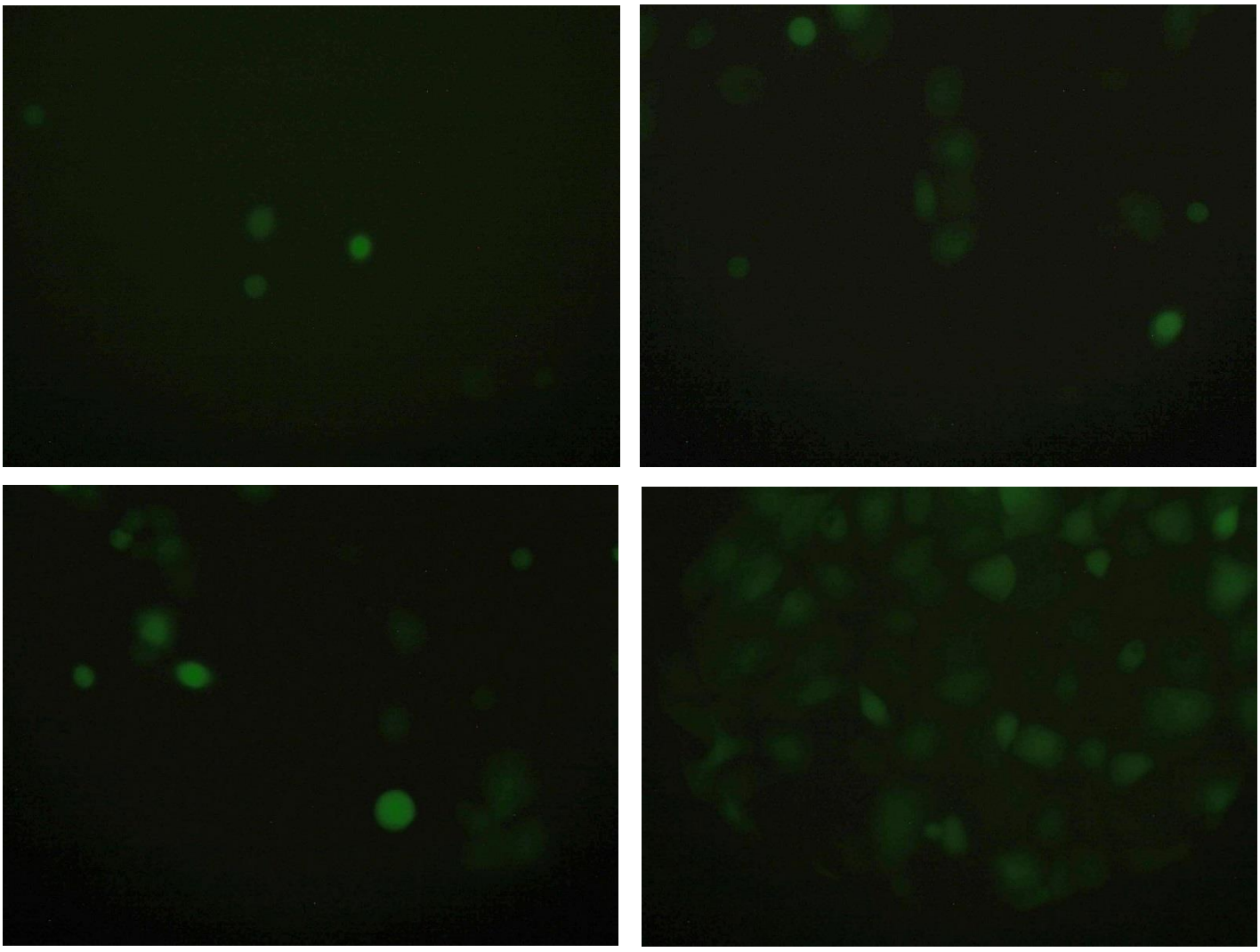

Fig. 27: Cellular populations at different concentrations, from left to right and top to bottom: $2.5 \cdot 10^5$, $3 \cdot 10^5$, $5 \cdot 10^5$, $1 \cdot 10^6$.

The second a third tests comprised the analysis of four populations.

The second one comprised the analyses of cell populations of $2.5 \cdot 10^5$, $5 \cdot 10^5$, $1 \cdot 10^6$ and $2 \cdot 10^6$ at frequencies from 1 kHz to 100 kHz in order to determine the frequency for which the system best responses and appears a bigger difference in the amplitudes of the samples.

Three different positions on the Petri dish are illuminated in this case, to determine also if there was a variation on the measures, which happened to be.

The third test comprised the analyses of $2.5 \cdot 10^5$, $3 \cdot 10^5$, $5 \cdot 10^5$ and $1 \cdot 10^6$ of cells at a greater number of intervals between the selected frequencies from 1 kHz to 100 kHz.

The measurements of amplitude in this two test were inconsistent and appeared to change with the position within the plate.

It was found that it was the illumination motif of the LED that was not proportioning a homogeneous illumination. Hence, a convergent lens was introduced in the system.

It was placed in between the emitter head and the sample at a distance that permits to illuminate it uniformly and at the same time as close as possible to it.

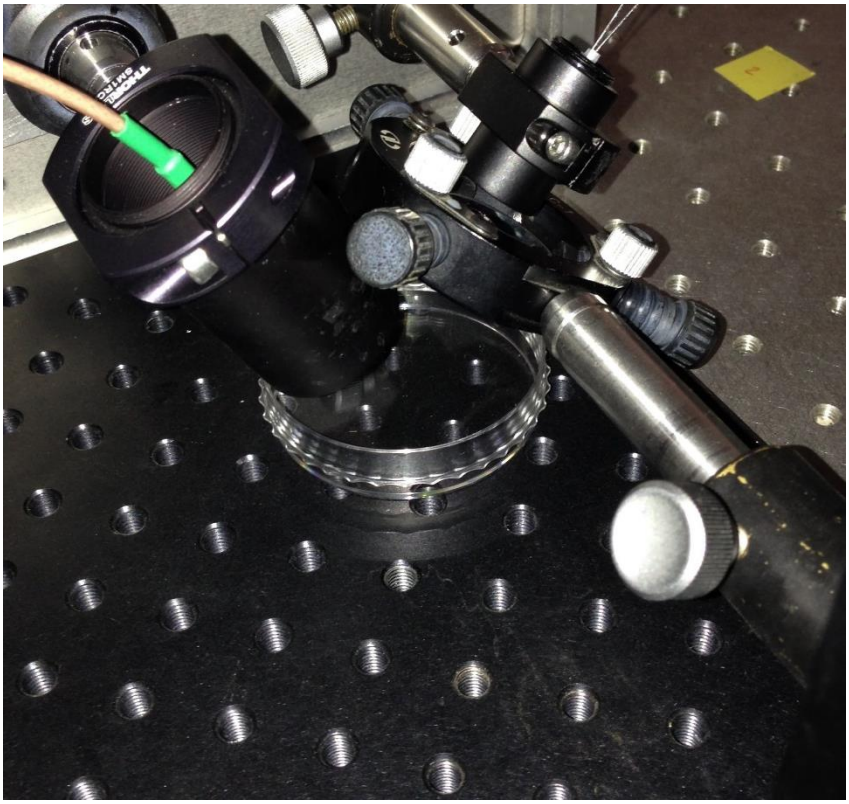

Fig. 28: Final optical setup

After this modification, a new test with cell concentrations of $2.5 \cdot 10^5$, $5 \cdot 10^5$, $1 \cdot 10^6$ and $2 \cdot 10^6$ from 10 to 50 kHz is carried out. The new amplitude measurements are smaller because the light of the LED is now placed further from the sample, but they are consistent and change as expected.

Measurements of just the Petri dish with the medium are also taken on each test, in order to process the data afterwards.

4.1. Experimental protocol to measure AEGs' fluorescence

Instrument assembly

The optical and mechanical parts of the system are changed in this case.

A LED is placed to excite the blood plasma samples at 325 nm and three filters for the collection of the emission at 380, 440 and 480 nm are placed on a wheel in front of the detector head. The common electronics remain the same.

Then, the blood plasma samples to be analyzed under the system are obtained

Obtaining and maintenance of blood plasma

The samples are provided by the Regenerative Medicine Unit of the Epithelial Biomedicine Group from the animal facility at CIEMAT.

The samples were taken from eight specimen of mus musculus (common mice). Four of them were healthy mice, two of them were diabetic-born and the other two were made diabetic by the repeated administration of streptozotocin according to the established procedures.

The samples were obtained from them arbitrary during a week, and they contained approximately 70 µl of blood. The blood was centrifuged in situ to obtain the blood plasma and then the samples were kept inside a portable freezer properly packed to be translated to the UC3M optoelectronics laboratory.

Data collection and analysis

The series of blood plasma samples obtained were analyzed in the same way under the system. Two different series of samples were obtained and analyzed on different days in order to check on the good functioning of the method.

The first series of samples was composed of two blood plasma samples of 172 mg/dl and 330 mg/dl.

In the first place, measures at the three different wavelengths of just the cuvette without any sample are taken, in order to characterize the reflectance of the measurements.

Afterwards, each sample is pipetted inside the cuvette at a time and the sample is excited at different frequencies from 1 kHz to 100 kHz in small intervals, with the purpose of obtaining the best response of the system. The emission of the sample is collected at three different wavelengths, by the selection of a band pass filter on each case.

In the second place, a first analysis of the collected data from these two samples was performed.
The measurements were normalized with the data obtained from the system reflectance. Afterwards, the calculation of the ratios between the amplitudes at different wavelengths was performed.

Three different ratios from the samples were obtained; a ratio of the intensities I_{380}/I_{440}, a ratio of the intensities I_{440}/I_{480} and a ratio of the intensities I_{380}/I_{480}.

The three ratios were compared among both samples. In the comparison of the ratio I_{440}/I_{480} (described as P_2/P_3 in some figures) it seemed that the two types of samples could be identified, because the one with a higher concentration in glucose had a bigger ratio than the one with a lower level, as expected. But it was too soon to reach valuable conclusions.

The good functioning of the detection needed to be checked with another series of samples, but since the measurements obtained appeared to be coherent, no modifications on the system were included.

The next series of samples were obtained an analyzed in the following day and they had a glucose concentration of 146 mg/dl and 542 mg/dl respectively.

The three amplitudes at the three wavelengths of emission were obtained, this time only for a frequency of 1 kHz.

Afterwards, the data was analyzed in the same way and was compared with the information obtained from the previous samples. From the comparison of the first ratio I_{380}/I_{440} among the two groups of samples, no relevant information could be obtained, as expected. Neither was found a relationship among the ratios I_{380}/I_{480}.

Then, the ratio among the two amplitudes related with the AEGs fluorescence were compared among the healthy or prediabetic and the diabetic individuals.

The ratio I_{440}/I_{480} permits to make a separation among the animals that are in the previous stages of the illness (normal and prediabetic) and the ones that already suffer from diabetes mellitus, as expected.

5. Results and conclusions

In this section, the results from the two applications assessed are presented. Also the principal conclusions of the development of the fluorescence spectroscopy device and the work involved in this project are discussed.

5.1. Results for the cell count estimation

In this section they are presented the results for the analysis of the different concentration of cells under the fluorescence spectroscopy instrument.

An analysis on the behavior of the system to the frequency of modulation was performed in order to find the frequency at which a major difference in the amplitude of the samples was appreciated.

As shown in the following chart, the best frequency to make a distinction among the samples was 20 kHz.

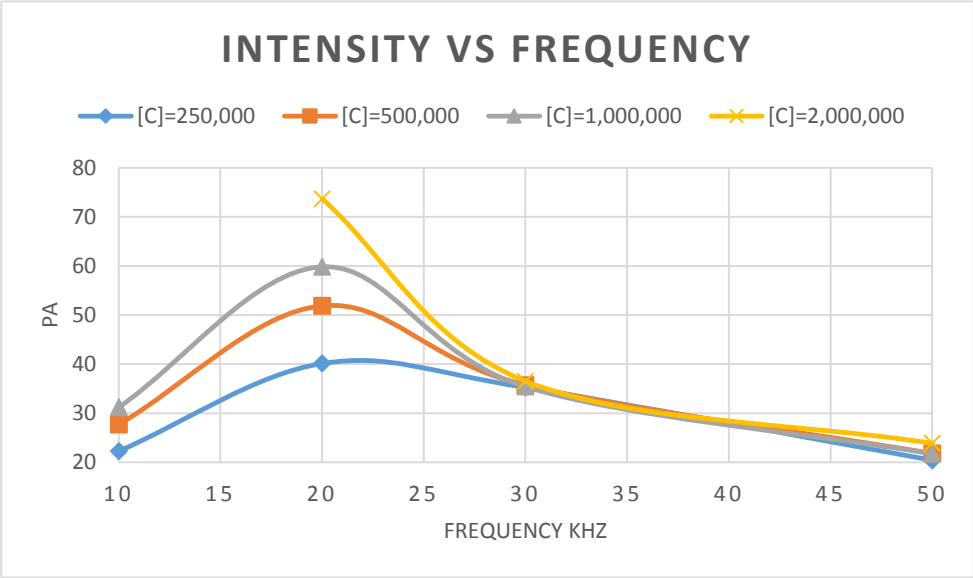

Fig. 29: System response to the emission of the cellular populations at different frequencies.

Hence, the difference in amplitudes from the samples were retrieved from the data at 20 kHz. They are presented in the following graph:

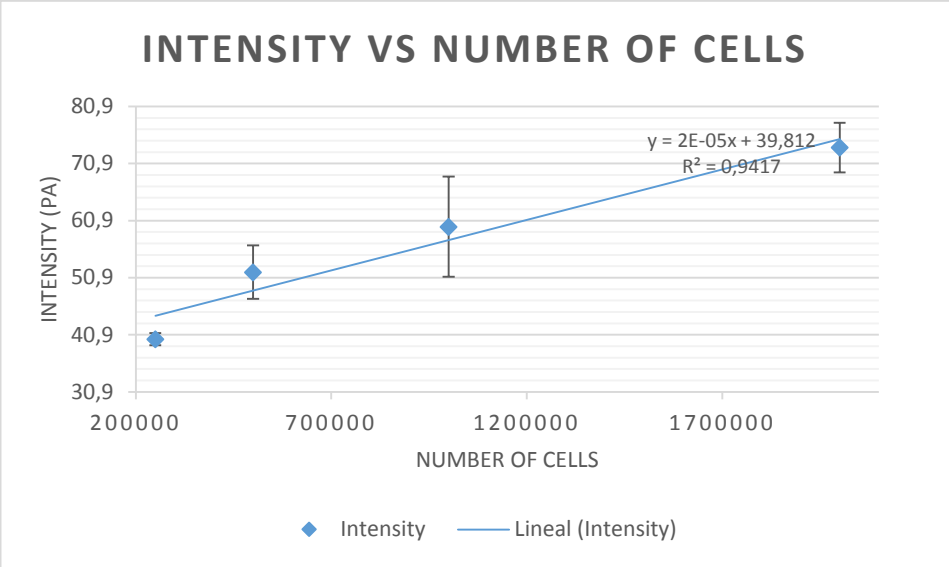

Fig. 30: Intensity vs. the number of cells in the sample. The intensity was obtained as the average of the intensities of three illuminated circular spots in the culture plate.

It is possible to appreciate in the following graph how does the intensity vary with the cell concentration under analysis. The greater the number of cell, the greater the number of fluorophores and hence the greater the detected intensity of fluorescence.

It has to be taken into account that the detected amplitude represented on this chart was not only due to the detection of fluorescence, but also due to the component of reflectance. Reflected light is also detected because the band-pass filters in the system are not ideal, and hence light at other wavelengths different from the one at the emission peak is being detected. The spectra are separated and narrowed as much as possible but this is not enough for the detection of just the fluorescence component.

The sensitivity of the system and the minimum number of cells that the system is able to detect were calculated and are presented in the following table:

CHARACTERISTICS	Calculation	Result	Units
Sensitivity	$\frac{Max.\ Intensity - Min.\ Intensity}{Max.\ No.\ of\ cells - Min.\ No.\ of\ cells}$	$1{,}9 \cdot 10^{-5}$	pA/cell
Min. No. of detected cells	$\frac{Standard\ deviation}{Sensitivity}$	16000 cells	

Table 1: The sensitivity and the minimum number of cells that is possible to detect with the system.

In the table, the second column includes the formulas to calculate both. The sensitivity is calculated as the slope of the curve. The minimum number of cells has been calculated as the ratio of the standard deviation and the sensitivity. The SD has been obtained from arbitrary measurements of the system's detection without any sample at equally spaced intervals of time.

5.2. Results for the AEGs' fluorescence detection

Here there are presented the results from the processing of the data from the fluorescence detection of AEGs.

The ratio from the intensities at 440 and 480 nm are obtained for each sample and represented on this graph, after being normalized.
It is noticeable that there exists a distinction among the ratio of the samples with a high glucose level, which is greater, and the samples with a lower glucose level, which is smaller.

Hence, providing a separation between the samples with a high glucose concentration (330 mg/dl and 542 mg/dl) and the samples with a low glucose concentration (146 mg/dl and 172 mg/dl).

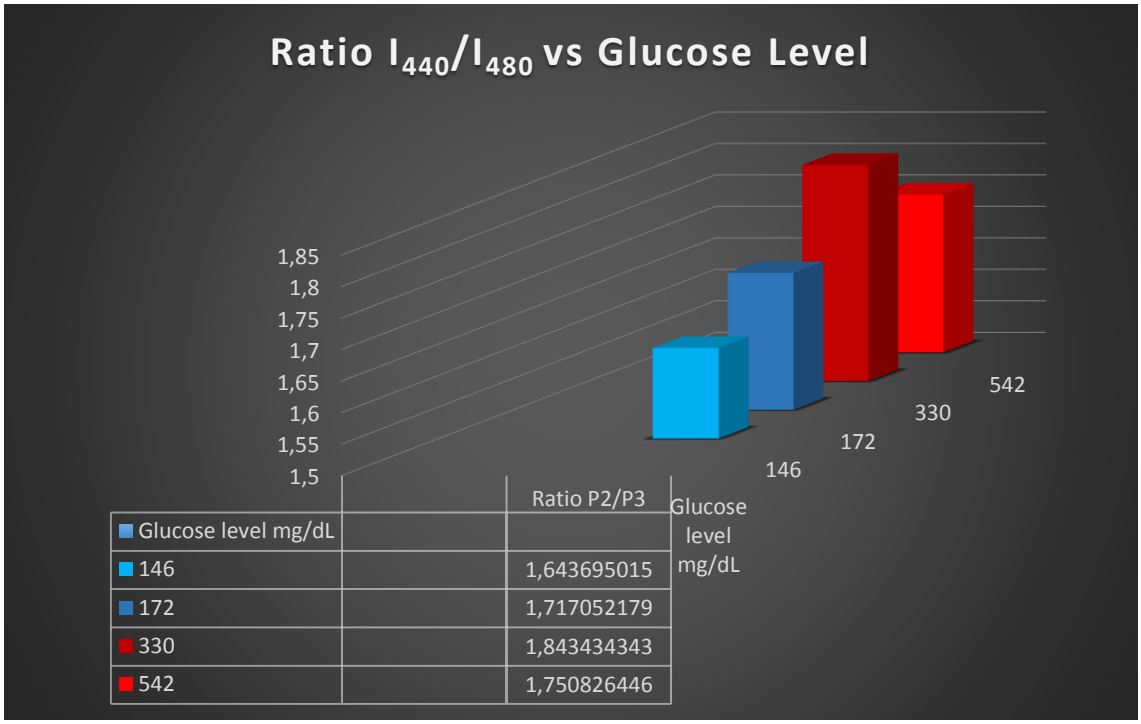

Fig. 31: Normal/prediabetic glucose levels (blue) and diabetic (red).

5.3. Conclusions

The fluorescence spectroscopy instrument that has been developed experimentally in this work is useful for both applications, the detection of the AEGs' fluoresce in the blood plasma and the GFP fluorescence in the cells.

The measurements obtained can be used to determine useful parameters from the samples under study. From the detection of the fluorescence of GFP, the number of cells or cellular concentration can be estimated.

In the same way, from the detection of the fluorescence related to AEGs it is possible to make a distinction between normal and abnormal levels of glucose in blood plasma.

Moreover, it is possible to make a more affordable and portable instrument, equivalent to the fluorescence spectroscopy system by substituting the components by equivalent compact circuits.The some costs related to the optics and mechanics of the system by making 3D-printed versions of the tube mounts and holders involved.

6. Bibliography

[1] Markus Sauer, Johan Hofkens, and Jörg Ederlein. *Handbook of Fluorescence Spectroscopy and Imaging: From Ensemble to Single Molecules*. Weinheim: WILEY-VCH Verlag & Co. KGaA, 2011. 1-280. Print.

[2] Cadena-Herrera, D., Esparza De Lara, J. E., López-Morales, N. A., Pérez, N. O., & Medina-Rivero, E. (2015, April). Validation of three viable-cell counting methods: Manual, semi-automated, and automated. *Biotechnology Reports, 7*. Retrieved from ScienceDirect (10.1016/j.btre.2015.04.004).

[3] Martín-Mateos, P., Crespo-Garcia, S., Ruiz-Llata, M., Lopez-Fernandez, J., Jorcano, J., Del Rio, M., & Acedo, P. (2014, September 1). Remote diffuse reflectance spectroscopy sensor for tissue engineering monitoring based on blind signal separation. *Biomedical Optics Express, 5*(9), 3231-3237.

[4] Shaw, K. M., & Cummings, M. H. (2012). *Diabetes: Chronic complications* (3rd ed., pp. 1-352). Oxford: John Wiley & Sons, Ltd.

[5] Diabetes (Fact Sheet Nº312). (2015, January). In *World Health Organization*. Retrieved September 12, 2015.

[6] Ortega, M. (2014, September 29). ¿Manejo inicial del diabético? Pan comido. In *Sapiens Medicus*. Retrieved September 14, 2015.

[7] Tébar Massó, F. J., & Escobar Jiménez, F. (2009). *La Diabetes Mellitus en la Práctica Clínica*. Madrid, Spain: EDITORIAL MÉDICA PANAMERICANA, S. A. Retrieved September 12, 2015.

[8] Han, S. (2014, September 29). How to Count Cells: An Overview of Cell Counting Methods. In *LinkedIn*.

[9] TC20™ Automated Cell Counter. (n.d.). In *Bio-Rad*. Retrieved September 14, 2015.

[10] Gaston College. (n.d.). Counting Cells Using a Hemocytometer. In *Learning Solutions*. Retrieved September 14, 2015.

[11] Beckman Coulter, Inc. - Particle Characterization. (n.d.). Using a Coulter Counter to Measure the Quality of Injectable Fat Emulsion. In *AZO Marerials*. Retrieved February 11, 2015.

[12] Ultra Violet (UV) Spectrophotometry. (n.d.). In *Bell International Laboratories: The Lab*. Retrieved September 14, 2015.pectrophotometer.

[13] College of Medicine, Biological Sciences and Psychology. (2014). Flow Cytometry. In *University of Leicester*. Retrieved September 14, 2015.

[14] Jahan-Tigh, R. R., Ryan, C., Obermoser, G., & Schwarzenberger, K. (2012). Flow Cytometry. *Journal of Investigative Dermatology, 132*. doi:10.1038/jid.2012.282.

[15] Chari Dingari, N., Horowitz, G. L., Woong Kang, J., Dasari, R. R., & Barman, I. (2012, February 29). Raman Spectroscopy Provides a Powerful Diagnostic Tool for Accurate Determination of Albumin Glycation. *PLoS ONE, 7*(2). doi:10.1371/journal.pone.0032406.

[16] Marques, M. P., Batista de Carvalho, L. A., & Haris, P. I. (2013). DCDR spectroscopy as an efficient tool for liposome studies: Aspect of preparation procedure parameters. In *Spectroscopy of Biological Molecules: Proceedings from the 14th European Conference on the Spectroscopy of Biological Molecules 2011* (pp. 99-103). Amsterdam, Netherlands: IOS Press.

[17] Cherkasova, O. P., Nazarov, M. M., Smirnova, I. N., Angeluts, A. A., & Shkurinov, A. P. (2014, July). Application of time-domain THz spectroscopy for studying blood plasma of rats with experimental diabetes. *Electromagnetic Applications In Biology And Medicine: Physics of Wave Phenomena*, *22*(3), 185-188. doi:10.3103/S1541308x14030042

[18] Brownlee, M., Vlassara, H., & Cerami, A. (1984, October 1). Nonenzymatic Glycosylation and the Pathogenesis of Diabetic Complications. *Annals of Internal Medicine*, *101*(4), 527-537. doi:10.7326/0003-4819-101-4-527

[19] Singh, Y. (2014). *Diabetes and Periodontum* (Doctoral dissertation, Yogender Singhdeswal).

[20] Papini, A. M., Nuti, F., Rovero, P., Larregola, M., Rentier, C., & Monasson, O. (n.d.). Synthesis of glycated and glycosilated peptides to detect autoantibodies in diabetic patient's sera. In *Peptlab*. Retrieved September 14, 2015.

[21] Shirshin, E., Cherkasova, O., Tikhonova, T., Berlovskaya, E., Priezzhev, A., & Fadeev, V. (2015, February 18). Native fluorescence spectroscopy of blood plasma of rats with experimental diabetes: identifying fingerprints of glucose-related metabolic pathways. *Journal of Biomedical Optics*, *20*(5). doi:10.1117/1.JBO.20.5.051033

[22] Lakowicz, J. R. (2006). *Principles of Fluorescence Spectroscopy* (3rd ed.). N.p.: Springer Science+Business Media, LLC

[23] Leiner, M. J., Schaur, R. J., Desoye, G., & Wolfbeis, O. S. (1986, July 10). Fluorescence topography in biology. III: characteristic deviations of tryptophan fluorescence in sera of patients with gynecological tumors. *Clinical Chemistry*, *32*(10), 1974-1978

[24] Suarez, G., Rajaram, R., Oronsky, A. L., & Gawinowic, M. A. (1988, February 25). Nonenzymatic Glycation of Bovine Serum Albumin by Fructose (Fructation): Comparison with the Maillard reaction initiated by glucose. *The Journal of Biological Chemistry*, *264*(7), 3674-3679.

[25] Tkachenko, N. V. (2006). *Optical Spectroscopy: Methods and Instrumentations* (pp. 1-322). Amsterdam, The Netherlands: Elsevier.

[26] FLIM. (n.d.). In *Olympus Biological Microscopes*. Retrieved September 14, 2015.

[27] *SR830 DSP Lock-In Amplifier User's Manual*, 1st ed. Standford Research Systems, Sunnyvale (California), 1993.

[28] Ruiz-Llata, M., Martín-Mateos, P., López, J. R., & Acedo, P. (2014, February). Remote optical sensor for real-time residual salt monitoring on road surfaces. *Sensor and Actuators*, *191*, 371-376.

[29] Martín Mateos, P. (2013). *Design and fabrication of a portable Diffuse Reflectance Spectroscopy instrument for skin vasculature assessment* (Master's thesis). 23 February.

[30] California Institute of Technology. (2014, August 6). Low-Noise Signal Detection with a Lock-In Amplifier. In *ALPhA*. Retrieved September 14, 2015.

[31] Lenti FAQs. (2015). In *SBI: Harnessing Innovation to Drive Discoveries*. Retrieved September 14, 2015.

[32] Laboratorio de Genómica Viral y Humana. (2011). Conteo y Evaluación de la Viabilidad de Células Mononucleares. In*Protocolos y métodos*. N.p.: Facultad de Medicina UASLP. Retrieved September 14, 2015.

[33] Celis, J. E. (2006). *Cell Biology: A laboratory handbook* (3rd ed., Vol. 2). San Diego, CA: Elsevier.

7. Annex

7.1 Project budget

Here it is going to be presented an estimation of the costs generated by this project.

Costs are presented divided in two main categories: personal costs, in the concept of time and knowledge invested by the participants; and material costs, which instead of including the equipment and instrumentation costs during the experimental work, it includes just the material costs that will be actually present in the generation of the instrument prototype.

Disclaims

This estimate merely includes the main costs, so other minor costs such as travel expenses and per diem expenses or consumables are not included.

There are some costs that are beyond the scope of this estimation, whose calculation is tedious or there is not enough information to determine them.

For this reason, the costs of the maintenance of the laboratories in which the work is carried out are not included.

Neither are the costs generated outside UC3M included in this section. Only costs in the university environment were estimated, although additional costs are generated outside (i.e.: the cost of the animals and the salary of the professionals at CIEMAT's animal facility).

Costs

In the following tables they are included the aforementioned costs. In Table 1, the names of the participants and their salary per hour according to their category is presented.

An estimation on the number of hours dedicated to the project is included and their estimated total salary for their involvement.

Personal Costs

PARTICIPANTS	Category	€/hour	Hours Spent	Total Costs
Pablo Acedo	Professor	300	52	15600 €
Pedro Martín	Doctor	36	100	3600 €
Laura Rey	Junior Engineer	20	240	4800 €
Marta García	Biologist	30	8	240 €
TOTAL BALANCE:				**24240 €**

Table 2: Participants and estimated invested time and salary.

In Table 2, the cost corresponding to the assembly of a future prototype (that were also present in the course of this work) are presented. The price of purchasing them was included in the first column.

The second column expresses their amortization time, as the months that they are expected to be useful until they cannot accomplish their function anymore or become obsolete.

The third column includes the time in months during which the devices were used in the course of this work. Finally, in the last column, the cost that they involved within this time is expressed. In order to obtain it, the amortization per month was calculated and this was multiplied by the number of months of use.

Cost of the Prototype

EQUIPMENT	Price	Amortization Period	Period of Use	Cost during the Period of Use
PC	1150	72	4	64 €
Laser driver	1917	240	4	32 €
Optical instrumentation				
- **LEDS**	404	72	4	25 €
- **Detector**	13	24	4	2 €
- **Filters**	574	120	4	19 €
- **Optical mounts**	300	240	4	5 €
TOTAL BALANCE				**147 €**

Table 3: Materials with its price and its estimated cost for the project. The periods of use and amortization of the equipment is included in months.

In the last table it is presented the total estimated cost of the project. It must be taken into account that the total cost could be reduced a lot by the substitution of the instrumentation and optical parts as explained before.

Total cost

Total Personal Costs	**24240 €**
Total Equipment Costs	**147 €**
FINAL COST	**24387 €**

Table 4: The sum of the personal and equipment costs represented in the final cost of the project